

ARIES

Accelerator Research and Innovation for European Science and Society

Horizon 2020 Research Infrastructures GA n° 730871

DELIVERABLE REPORT

[Evaluation of cleaning process]

DELIVERABLE: D15.1

Document identifier:	ARIES_Deliverable D15.1.docx
Due date of deliverable:	End of Month 12 (May 2018)
Justification for delay:	The coating systems set up required more time than what previously scheduled
Report release date:	31/05/2018
Work package:	WP15: Thin Film for Superconducting RF Cavities (TF-SRF)
Lead beneficiary:	INFN
Document status:	Draft

ABSTRACT

The goal of the deliverable D15.1 is to define an optimum cleaning and polishing procedure for the surface preparation of Cu in order to minimize the substrate effect on the final properties of Nb film coating. The optimum cleaning and polishing process is defined through the evaluation of the superconductive properties of Nb thin film coated on copper planar samples that are cleaned and polished with different procedures. In this framework 5 different procedures were investigated for a total amount of 50 samples prepared. Nb thin film deposition was done on each sample using the same procedure and parameters. Several surface and superconductive characterizations were done to evaluate the effect of the surface preparation on Nb film properties. Based on the results of the WP15 first year work, we concluded that the samples for task 15.3, will be prepared by 2 techniques only: EP, as a pitting free technique, and SUBU, as the techniques which provides the lowest roughness without scratches.

ARIES Consortium, 2018

For more information on ARIES, its partners and contributors please see <http://aries.web.cern.ch>

This project has received funding from the European Union's Horizon 2020 Research and Innovation programme under Grant Agreement No 730871. ARIES began in May 2017 and will run for 4 years.

Delivery Slip

	Name	Partner	Date
Authored by	C. Pira	INFN	31/05/18
	C. Antoine	CEA-Saclay	
	A. Katasevs	RTU	
	O. Kugeler	HZB	
	A. Medvids	RTU	
	E. Seiler	IEE Bratislava	
	A. Sublet	STFC	
	R. Valizadeh	CERN	
	M. Vogel	UniSIEGEN	
	O. Malyshev	STFC	
Edited by	C. Pira	INFN	31/05/18
Reviewed by	C. Pira [Task coordinator]	INFN	31/05/18
	O. Malyshev [WP coordinator]	STFC	
	S. Guiducci [Scientific coordinator]	INFN	
Approved by	M. Vretenear		dd/mm/yy
	Steering Committee		

TABLE OF CONTENTS

1. INTRODUCTION.....	5
2. SAMPLE PREPARATION (TASK 15.2)	6
2.1 SAMPLE PRODUCTION	6
2.2 SUBU CHEMICAL POLISHING	6
2.2.1 <i>SUBU Cleaning Procedure at CERN.....</i>	<i>7</i>
2.2.2 <i>SUBU Cleaning Procedure at INFN.....</i>	<i>8</i>
2.2.3 <i>SUBU Surface Characterization at INFN.....</i>	<i>9</i>
2.3 ELECTROPOLISHING.....	12
2.3.1 <i>EP Cleaning Procedure at INFN.....</i>	<i>13</i>
2.3.2 <i>EP Surface Characterization at INFN.....</i>	<i>14</i>
2.4 EP+SUBU	16
2.4.1 <i>EP+SUBU Cleaning Procedure at INFN.....</i>	<i>16</i>
2.4.2 <i>EP+SUBU Surface Characterization at INFN.....</i>	<i>16</i>
2.5 TUMBLING	18
2.5.1 <i>Tumbling Cleaning Procedure at INFN.....</i>	<i>18</i>
2.5.2 <i>Tumbling Surface Characterization at INFN.....</i>	<i>19</i>
2.6 LASER POLISHING AT RTU	21
2.7 SURFACE CHARACTERIZATION COMPARISON	23
3. NB FILM DEPOSITION (TASK 15.3)	24
3.1 SAMPLE DEPOSITION AT STFC.....	25
3.1.1 <i>STFC Nb film Surface Characterization.....</i>	<i>26</i>
3.2 SAMPLE DEPOSITION AT SIEGEN.....	27
3.2.1 <i>Siegen Nb film Surface Characterization.....</i>	<i>28</i>
3.3 SAMPLE DEPOSITION AT INFN	32
3.3.1 <i>INFN Nb film Surface Characterization.....</i>	<i>32</i>
3.4 FILM CHARACTERISATION WITH THERMAL ELECTRON AND EXOELECTRON EMISSION AT RTU	37
4. SC PROPERTIES EVALUATION AT IEE (TASK 15.4)	40
5. DISCUSSION.....	43
5.1 EXPECTED CONSEQUENCES FROM SURFACE MORPHOLOGY ON RF PERFORMANCE.....	43
6. CONCLUSIONS AND FUTURE WORK	46
REFERENCES	47
ANNEX: GLOSSARY.....	49

Executive summary

Goal of deliverable 15.1 is to find an optimum cleaning and polishing process for copper through the evaluation of the superconductive properties of Nb thin films coated on copper planar identical substrates that are cleaned and polished with different procedures. In this framework 5 different procedures were investigated for a total amount of 50 samples prepared.

The cleaning and polishing procedures were carried out at CERN and INFN. At CERN 25 copper planar samples were treated with SUBU solution as reference, at INFN other 25 samples were divided in 4 different batches, one for each treatment investigated: SUBU solution, EP, SUBU+EP and Tumbling. On 6 polished CERN samples, a laser polishing was also performed at RTU, for a total of 5 different cleaning and polishing treatments.

A slight difference has been observed between different surface preparations. EP provides a pitting free surface, but the lowest roughness has been obtained with SUBU and tumbling. Initial exploration on laser polishing shows that it removes larger roughness and scratches; further investigation is required before deposition.

On 15 out of the 50 treated copper planar samples, a 3 μm thick Nb film deposition was done. The deposition processes were carried out at STFC, University of Siegen and INFN, 5 samples each, using the same procedure and parameters. Samples treated in the same cleaning and polishing batch were coated in more than one laboratory, in order to minimize the role of deposition facility on the SC film properties.

Different surface characterizations have been applied in order to compare the impact of different substrate preparations on films' sc properties: roughness measurements, SEM, EDS, XRD, AFM, and thermal and photo-stimulated exoelectrons measurements, in 4 different institutions (INFN, Siegen, STFC, RTU).

Superconducting properties of Nb films were evaluated with PPMS at IEE. It shows a slight difference between deposition facilities rather than different surface preparation; rf test will be required in future to assess the final choice.

The obtained results are encouraging further exploration on structural and sc characterizations, in order to discover the exact source of variation. This work will continue next year within Task 15.2. Based on the results of the first-year work, we concluded that the samples for task 15.3, will be prepared by 2 techniques only: EP, as a pitting free technique, and SUBU, as the techniques which provides the lowest roughness without scratches.

1. Introduction

ARIES WP15 ambition is to improve the performances of superconducting (SC) cavities by coating techniques. Thin films of Nb₃Sn on Nb and Nb on Cu are the solutions that will be explored. Thin film technology moves the surface preparation from Nb to Cu, because the Nb thin film cannot be chemical treated. For the Nb on Cu resonant cavities two principal copper cleaning and polishing treatments were studied: one is the electropolishing and the other one is the chemical polishing with SUBU solution [1] [2] [3] [4]. The influence of surface preparation is deeply studied in bulk Nb cavities and it is responsible for the main performances advancement. Similar considerations can be done for Nb/Cu cavities, because the morphology and the roughness of the copper surface are replicated by the Nb growing film. Moreover, there exist studies that show a direct correlation between copper surface preparation and Nb films SC properties [5]. A better understanding of the surface effects and their impact on the thin film and later on rf-properties of the coating is mandatory in order to reach the final goal of ARIES WP15 and it is the scope of the present deliverable.

Operatively the deliverable consists in the definition of cleaning and polishing process for copper samples, that will be further processed in task 15.3. The optimum cleaning and polishing process is defined through the evaluation of the superconductive properties of Nb thin film coated on the copper planar samples that are cleaned and polished with 4 different procedures.

The cleaning and polishing procedures were carried out at CERN and INFN. At CERN 25 copper planar samples were treated with SUBU solution as reference, at INFN other 25 samples were divided in 4 different batches, one for each treatment investigated: SUBU solution, EP, SUBU+EP and Tumbling. On 6 polished CERN samples, a laser polishing was also performed at RTU, for a total of 5 different cleaning and polishing treatments.

On 15 out of the 50 treated copper planar samples, a 3 μm thick Nb film deposition was done. The deposition processes were carried out at STFC, University of Siegen and INFN, 5 samples each, using the same procedure and parameters. Samples treated in the same cleaning and polishing batch were coated in more than one laboratory, in order to minimize the role of the deposition facility on the SC film properties.

Surface characterization on Cu samples and Nb film was done after each process (polishing, film coating, post treatment, etc.), directly by the partner involved in the process. At this stage, superconductive characterizations were carried out at IEE Bratislava and consist in an ac susceptibility characterization. Next year, more superconductive characterizations will be done at CEA-Saclay with a local AC-magnetometer, at STFC with a radiofrequency cathode and at HZB and CERN on QPR's sample in order to have more information about the correlation between polishing treatment and superconductive properties.

2. Sample preparation (task 15.2)

The sample preparation is divided in 2 principal phases: the sample production made at CERN and the sample polishing, carried out at CERN and at INFN. The polishing procedures were carried out at CERN and INFN. At CERN 25 copper planar samples were treated with SUBU solution as reference, at INFN other 25 samples were divided in 4 different batches, one for each treatment investigated: SUBU solution, EP, SUBU+EP and tumbling. For all the processes, except tumbling, 40 µm of material removing was agreed on in order to have comparable results. Unlike chemical and electrochemical polishing, tumbling smooths the surface without etching. A surface characterization was done at INFN after each treatment and consists of roughness evaluation, SEM and ESD analysis.

2.1 SAMPLE PRODUCTION

During the WP15 kick-off meeting it was decided that all samples for the 1st year programme should be produced from the same sheet of OFE copper. Following this plan, 50 samples with a size of 53mm x 53 mm were cut at CERN from the same copper sheet.

- 25 samples have been sent to INFN for cleaning and treatment
- 25 samples remained at CERN for cleaning and treatment

2.2 SUBU CHEMICAL POLISHING

Chemical polishing with SUBU is a standard process in the copper cavity preparation of all Nb/Cu SRF accelerators realized until now [1] [2] [3] [4].

Chemical polishing is easier and cheaper than electropolishing and, mostly, it is not affected by geometry, since no electric field is needed: the dissolution process is driven only by chemical reactions. The polishing agent is SUBU5, a solution developed for LEP2 at CERN [6] [7] [8]. SUBU5 is a mixture of sulfamic acid (5g/l), hydrogen peroxide 32% (50ml/l), n-butanol 99% (50ml/l) and ammonium citrate (1g/l) and the working temperature is around 72°C. After SUBU the cavity is passivated for 1-3 minutes with an aqueous solution 20g/l of sulfamic acid and then rinsed in deionized water. It is very important to carry out the passivation task as fast as possible, in order to prevent oxidation.

There are not so many works on SUBU polishing mechanism. The role of each component of the solution is reported in an internal CERN report [9]. Sulfamic acid, at 70 °C, in the presence of an oxidant (H₂O₂), forms with the copper a copper sulfamate. Oxygen peroxide generates active oxygen and dissolves the copper. Ammonium citrate is a moderator of the reaction, it limits the pitting process on the surface. N-butanol limits the bubble production.

2.2.1 SUBU Cleaning Procedure at CERN

1. Degreasing: in NGL 1740 bath for about 2 hours, with 3-5 minutes ultra-sonic ON at start and again 3 minutes ultra-sonic ON before end.
2. Activation: sulfamic acid (H_3NO_3S , 5 g/l) for about 3 minutes in order to increase surface wettability and avoid bubbling formation at the surface.
3. Polishing: 40 minutes "SUBU5", SUBU5 = sulfamic acid (H_3NO_3S , 5 g/l), hydrogen peroxide (H_2O_2 , 5% vol), n-butanol (5% vol) and ammonium citrate (1 g/l) at $72^{\circ}C$ ($70-75^{\circ}C$) with bath agitation, 5 samples in a 10L beaker.
4. Pre-rinsing with acid: sulfamic acid (H_3NO_3S , 5 g/l) for about 1 minute, to remove hydrophobic layer.
5. Rinsing with water: demineralized water for about 30 seconds.
6. Spraying with alcohol: ethyl alcohol to enhance drying.
7. Drying with N_2 .
8. Packing in wafer box.
9. Then in plastic bag under N_2 .

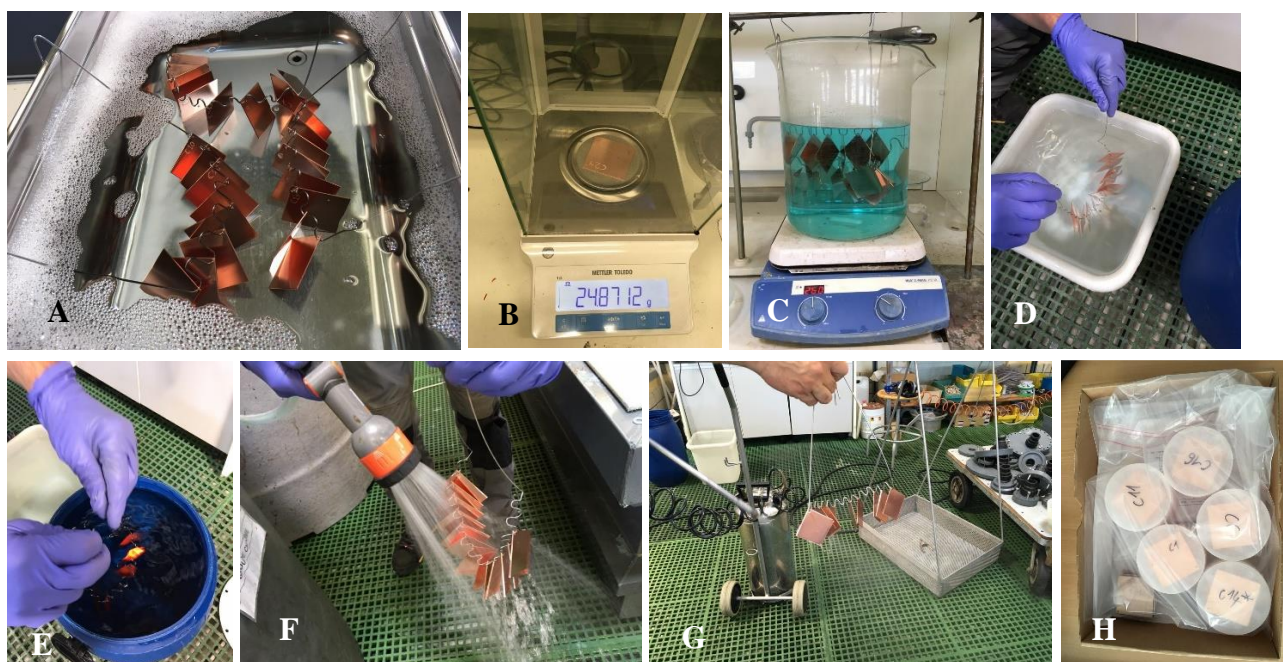


Figure 1 Pictures of the different phases of the SUBU polishing procedure. A) Degreasing, B) Weighting, C) SUBU Polishing, D) Pre-rinsing with sulfamic acid, E) and F) Rinsing with water, G) Spraying with alcohol, H) Packing in wafer box

As the etching rate was low due to the large surface of samples with respect to bath volume, steps 2 to 8 were repeated in two different batches (13 and 12 samples each respectively) of 40 minutes in order to remove more material. After first SUBU (SUBU#1) and based on two samples weighting before/after (C24 and C25, with a micro-balance - resolution down to $0.1 \mu g$) the average polished thickness was = $14.3 \mu m$.

After second SUBU with 13 samples (SUBU#2.1) it was = $19.4 \mu m$

And finally for the second SUBU with 12 samples (SUBU#2.2) it was = 24.4 μm

Total average etched thickness = 33.7 μm for batch 1 and 38.7 μm for batch 2, close to the agreed 40 μm .

Only the CERN spare samples were used for weighting, all the others remained untouched.

2.2.2 SUBU Cleaning Procedure at INFN

5 samples composed the SUBU batch. The procedure is the following:

1. Degreasing: in NGL 1740 bath for about 2 hours, with 3-5 minutes ultra-sonic ON at start and again 3 minutes ultra-sonic ON before end.
2. Activation: sulfamic acid ($\text{H}_3\text{NO}_3\text{S}$, 5 g/l) for about 3 minutes in order to increase surface wettability and avoid bubbling formation at the surface.
3. Polishing: 30 minutes "SUBU5", SUBU5 = sulfamic acid ($\text{H}_3\text{NO}_3\text{S}$, 5 g/l), hydrogen peroxide (H_2O_2 , 5% vol), n-butanol (5% vol) and ammonium citrate (1 g/l) at 72°C (70-75°C) with bath agitation, 5 samples in a 5L beaker.
4. Pre-rinsing with acid: sulfamic acid ($\text{H}_3\text{NO}_3\text{S}$, 5 g/l) for about 1 minute, to remove hydrophobic layer.
5. Rinsing with water: demineralized water for about 30 seconds.
6. Spraying with alcohol: ethyl alcohol to enhance drying.
7. Drying with N_2 .
8. Polishing: 35 minutes "SUBU5", SUBU5 = sulfamic acid ($\text{H}_3\text{NO}_3\text{S}$, 5 g/l), hydrogen peroxide (H_2O_2 , 5% vol), n-butanol (5% vol) and ammonium citrate (1 g/l) at 72°C (70-75°C) with bath agitation, 5 samples in a 5L beaker.
9. Pre-rinsing with acid: sulfamic acid ($\text{H}_3\text{NO}_3\text{S}$, 5 g/l) for about 1 minute, to remove hydrophobic layer.
10. Rinsing with water: demineralized water for about 30 seconds.
11. Spraying with alcohol: ethyl alcohol to enhance drying.
12. Drying with N_2 .
13. Packing in wafer box.
14. Then in plastic bag under N_2 .

The procedure, in this case, is exactly the same used at CERN for the first 25 samples, except the process time. The SUBU erosion rate strongly depends on the sample surface / solution volume ratio. To have comparable results we fixed the total etched thickness. The thickness of removed material is set to be $40 \pm 5 \mu\text{m}$ for all the INFN samples except the 8 treated in the tumbling batch.

The SUBU5 solution of step 8 is a fresh solution.

After first SUBU (before point 8) and based on two samples weighted before/after (L2 and L20, with a micro-balance - resolution down to 0.1 μg) the average etched thickness was = 18.8 μm .

After second SUBU it was = $21.0 \pm 0.06 \mu\text{m}$

Total average etched thickness = $39.8 \pm 0.06 \mu\text{m}$.

2.2.3 SUBU Surface Characterization at INFN

Only the INFN spare samples were used for weighting and characterization, all the others remained untouched. 5 different characterizations were done:

- a) Optical Inspection
- b) Reflectivity
- c) Roughness
- d) SEM
- e) EDS

Optical Inspection and Reflectivity measure

The substrate presents a mirror like surface (Figure 2).

The reflectivity was measured with a Portable Konica Minolta Spectrophotometer 2600d (Figure 3) and integrated in the wavelength range 400-700 nm.

Reflectivity (400-700 nm): 65.0 ± 0.3 %.

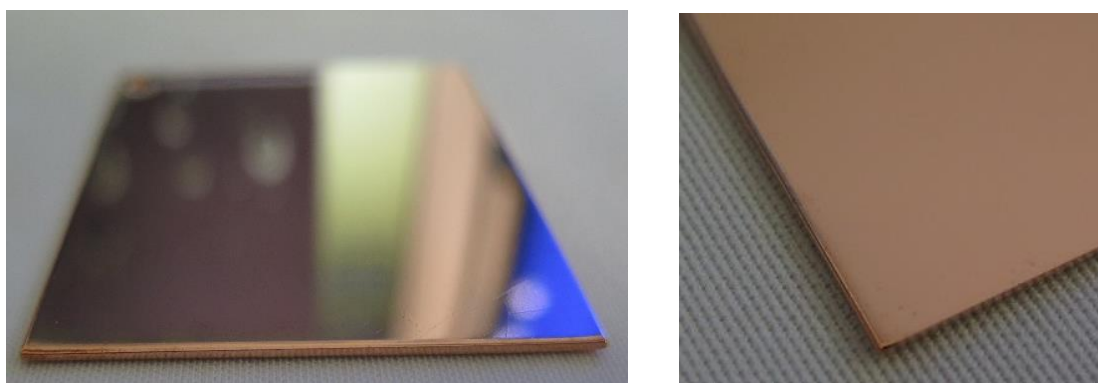


Figure 2 Pictures of a planar sample treated with SUBU process



Figure 3 Set-up for the Reflectivity characterization

Roughness

The roughness was measured with a Veeco Dektat 8 profilometer, using the following parameters: Scan length: 1 mm, applied force 12 mg. 3 scans on 2 different directions (a total of 6 scans) have been done in order to take into account the roll forming effect.

Initial (average values on 6 samples), Ra = 130 ± 30 nm

After SUBU (average values on 2 samples), Ra = 52 ± 8 nm

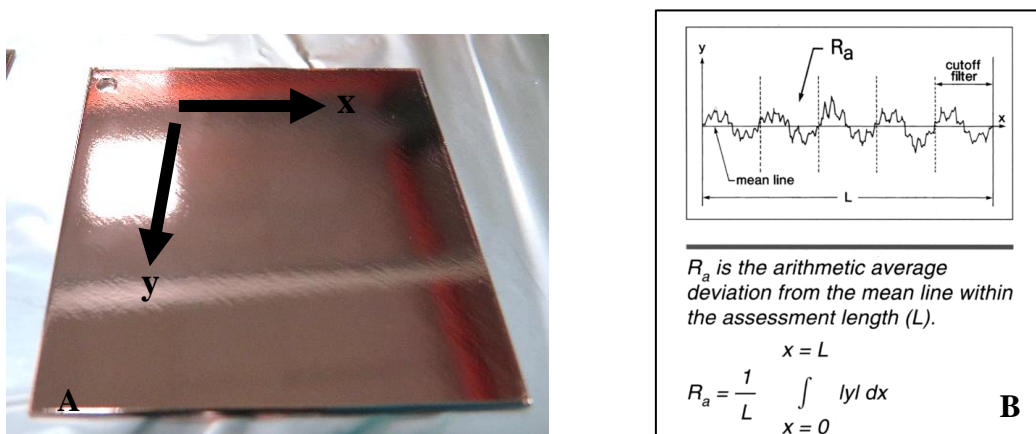


Figure 4 A) Roughness scan directions, B) Roughness definition

SEM and EDS

A Philips XL 30 as SEM and a Bruker X-Lash Detector 410-M for the EDS analysis it have been used.

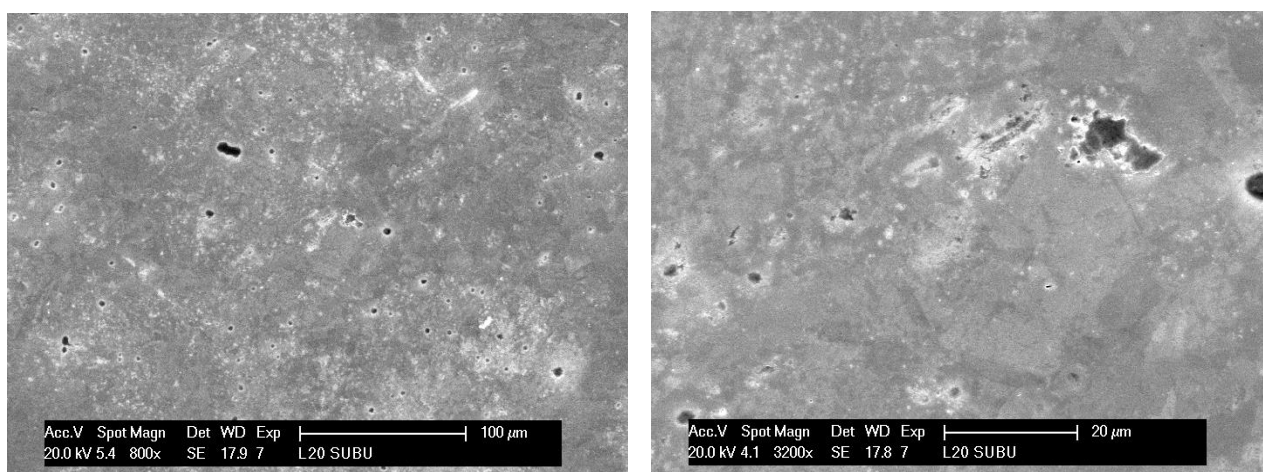


Figure 5 SEM micrographs at two different magnification level of a SUBU treated sample

The SEM characterization reveals the presence of pitting on the surface due to SUBU process.

EDS characterization was also done. The untreated substrate shows only the peaks of copper, as it is expected from OFHC copper. After SUBU no visible contaminations appear.

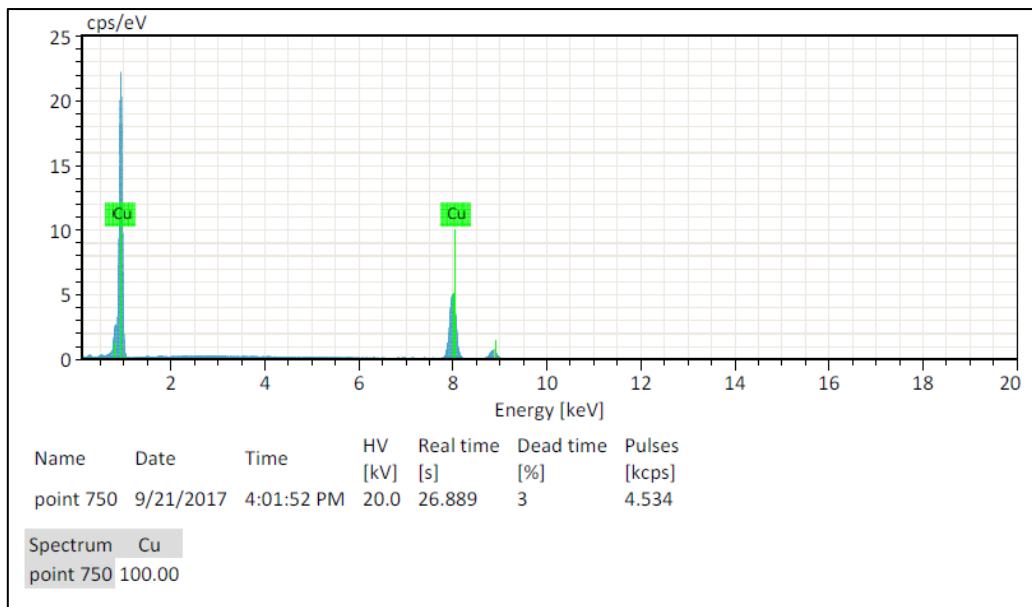


Figure 6 EDS analysis on the untreated sample

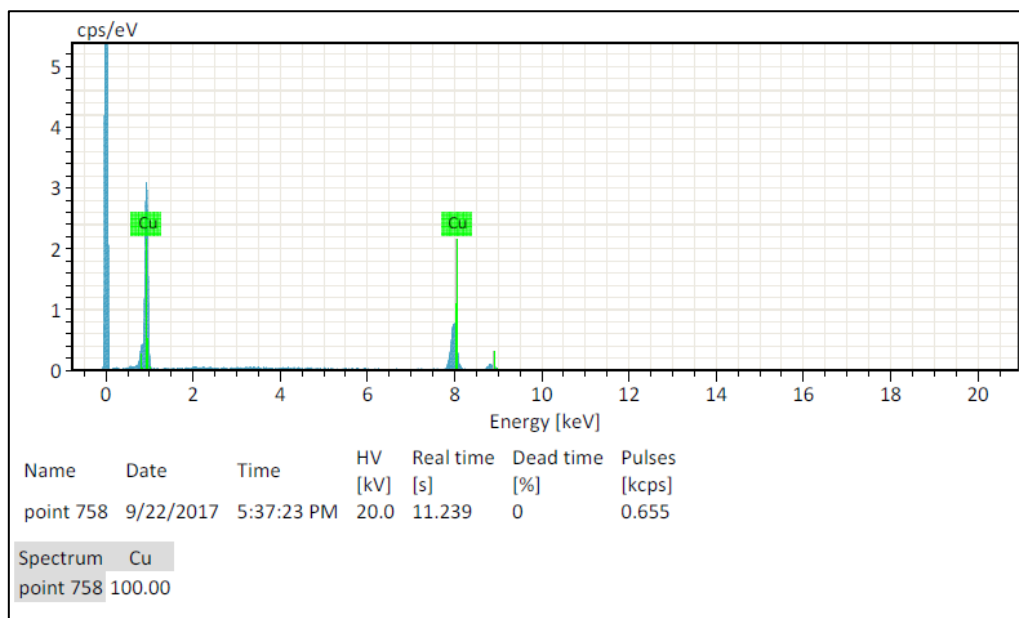


Figure 7 EDS analysis on a SUBU treated sample

2.3 ELECTROPOLISHING

The second treatment evaluated in this work is ElectroPolishing (EP). In the electrolytic cell the anode (+) is the copper cavity and the cathode (–) is made from pure copper. The electrolyte is a mixture of phosphoric acid and butanol in a volume ratio of 2 : 3. In a review of the copper electropolishing mechanism [10] several hypotheses were analysed to explain the mechanism of electropolishing of Copper in phosphoric acid solutions. All of them concern the existence of a thin bluish viscous layer of electrolyte forming in proximity of the anode, where oxidation reaction and copper dissolution occur. In a simple one, the thickness of such a film influences the erosion rate. On the protrusions, the film is thinner than the surrounding valleys. Hence, protrusions dissolve more rapidly than valleys. Another hypothesis starts from a simple geometrical consideration: the electric field has higher intensity at corners, edges and protuberances than at wells, cavities and craters. Surface levelling occurs as a result of greater dissolution probability of peaks. One of the key parameters characterizing the EP process is the current (I) – voltage (V) characteristic curve [11] (Figure 8). It shows the ideal and typical I–V characteristics for EP [10]. Depending on the voltage applied, it is possible to obtain pitting, polishing, or gas evolution. For voltages less than V_b , the surface preserves its mechanically worked appearance and shows some signs of pitting. This region is not recommended for EP. Just above V_b , there occur fluctuations in both voltage and current and a simultaneous drop in current density. Between V_b and V_c , a current plateau appears, usually attributed to diffusion-limited phenomena. Over the plateau, the current density remains constant even though the voltage increases. A polishing effect is observed between V_b and V_c , but the best results are obtained near point V_c . The first bubbles of gaseous oxygen appear on the anode at V_c . At higher voltages, evolution of oxygen accompanies the dissolution of metal, and pitting may occur due to oxygen bubbles trapped on the anode surface. The current density is inversely proportional to viscosity of the layer. Moderate agitation of the electrolyte reduces the thickness of the viscous layer so the current density increases, and the voltage drops. Vigorous agitation reduces the thickness to a few tenths of a millimeter and voltage drops even more. However, intense stirring gives a rougher surface finishing rather than polished [11]. Other important parameters are the electrolyte temperature, the acid concentration and the solution viscosity.

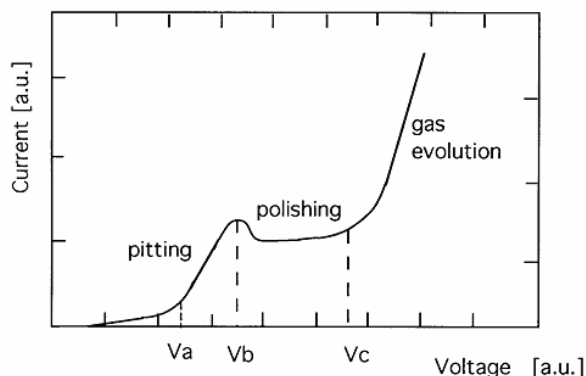


Figure 8 Current density vs. voltage for Copper electropolishing in phosphoric acid [10].

2.3.1 EP Cleaning Procedure at INFN

8 samples composed the EP batch. The procedure is the following:

1. Degreasing: in NGL 1740 bath for about 2 hours, with 3-5 minutes ultra-sonic ON at start and again 3 minutes -ultra-sonic ON before end.
2. Activation: sulfamic acid (H_3NO_3S , 5 g/l) for about 3 minutes in order to increase surface wettability and avoid bubbling formation at the surface.
3. Polishing: Electropolishing in a solution composed by Phosphoric Acid (H_3PO_3 85%) and Buthanol ($C_4H_{10}O$ 99%) in a ratio 3:2, at room temperature, without bath agitation.
4. Pre-rinsing with acid: sulfamic acid (H_3NO_3S , 5 g/l) for about 1 minute to remove hydrophobic layer.
5. Rinsing with water: demineralized water for about 30 seconds.
6. Spraying with alcohol: ethyl alcohol to enhance drying.
7. Drying with N_2 .
8. Pre-rinsing with acid: sulfamic acid (H_3NO_3S , 5 g/l) for about 1 minute, to remove hydrophobic layer.
9. Rinsing with water: demineralized water for about 1 minute.
10. Spraying with alcohol: ethyl alcohol to enhance drying.
11. Drying with N_2 .
12. Packing in wafer box.

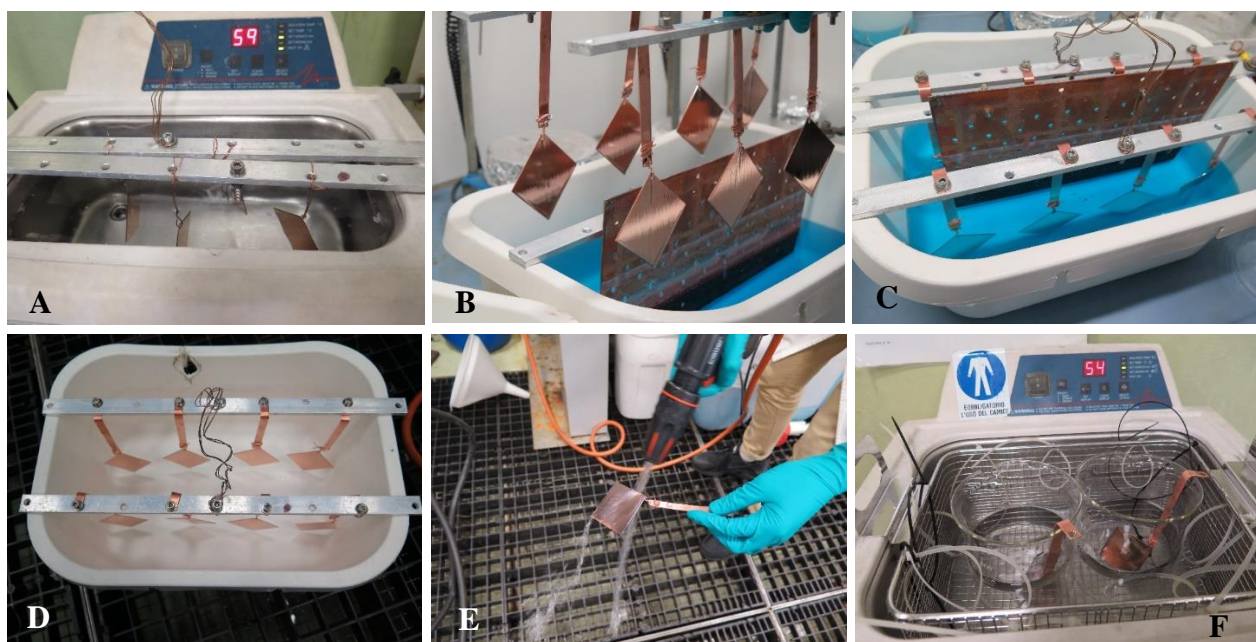


Figure 9 Pictures of the different phases of the EP polishing procedure. A) Degreasing, B) and C) EP Polishing, D) Pre-rinsing with sulfamic acid, E) and F) Rinsing with water

The etched thickness is controlled by the total amount of charge passed during the EP process and by samples weighting. Average etched thickness is based on two samples weighted before/after process (L21 and L22, with a micro-balance - resolution down to $0.1 \mu g$).

Total average etched thickness = $40 \pm 2 \mu m$.

The samples were sent to WP15 partners for the Nb deposition on October 2017.

2.3.2 EP Surface Characterization at INFN

Optical Inspection and Reflectivity measure

The substrate presents a **mirror like surface with a diagonal texture** (Figure 10) due to the oxygen evolution during the EP process. The texture could be reduced introducing and optimizing a bath agitation.

Reflectivity (400-700 nm): **64 %**.

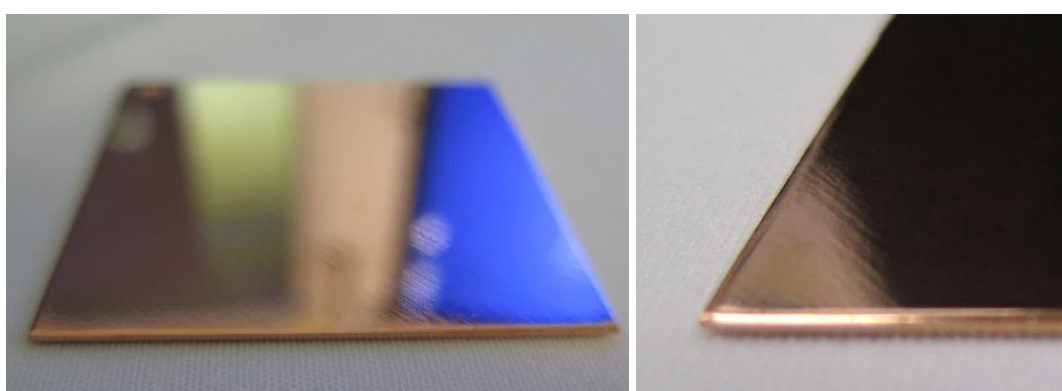


Figure 10 Pictures of a planar sample treated with EP process

Roughness

Initial surface (average values on 6 samples), $R_a = 130 \pm 30$ nm

After EP (average values on 2 samples), $R_a = 225 \pm 80$ nm

The roughness value is strongly influenced by the EP texture. The roughness measured parallel to the texture (blue arrow on Figure 11) is almost 3 times lower than the one measured along x and y directions.

After EP (scan along the diagonal direction), $R_a = 86 \pm 14$ nm

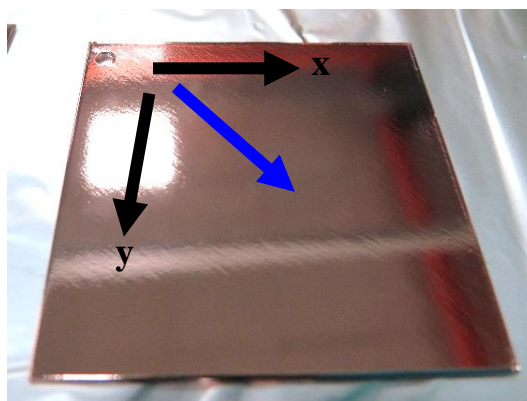


Figure 11 Roughness scan directions

SEM and EDS

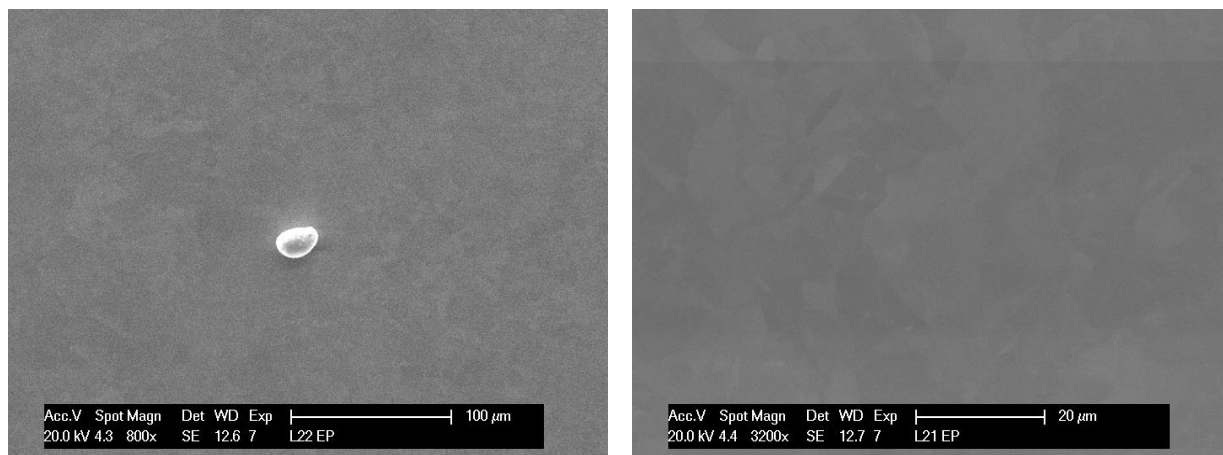


Figure 12 SEM micrographs at two different magnification level of an EP treated sample

The SEM characterization shows a very smooth surface. No pitting is visible. EDS characterization was also done. After EP no visible contaminations appear.

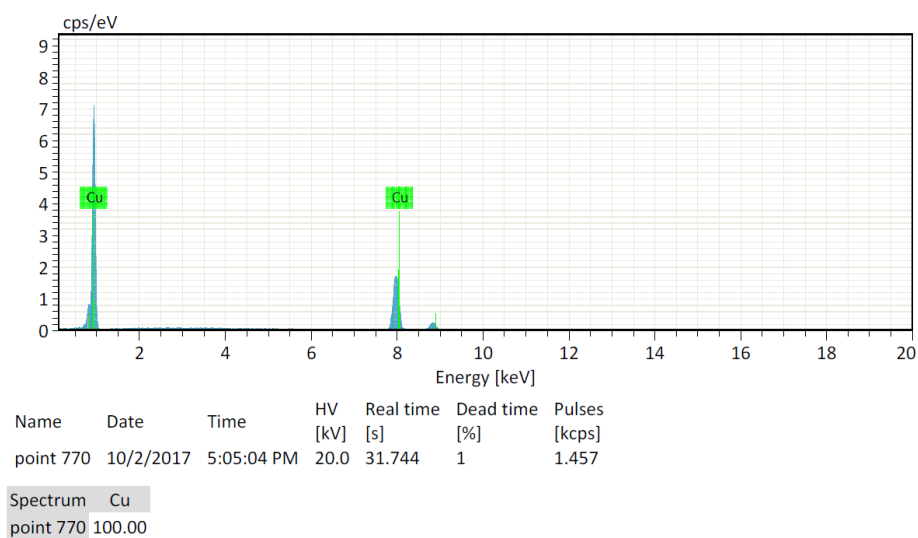


Figure 13 EDS analysis on an EP treated sample

2.4 EP+SUBU

On ALPI linac and LHC cavity surface preparation, a double process was used. First a deeply etching with EP and then a SUBU for the surface finishing [1] [3].

2.4.1 EP+SUBU Cleaning Procedure at INFN

5 samples composed the EP+SUBU batch. The procedure is the following:

1. Degreasing: in NGL 1740 bath for about 2 hours, with 3-5 minutes ultra-sonic ON at start and again 3-ultra-sonic ON before end.
2. Activation: sulfamic acid (H_3NO_3S , 5 g/l) for about 3 minutes in order to increase surface wettability and avoid bubbling formation at the surface.
3. Polishing: Electropolishing in a solution composed by Phosphoric Acid (H_3PO_3 85%) and Buthanol ($C_4H_{10}O$ 99%) in a ratio 3:2, at room temperature, without bath agitation.
4. Rinsing with water: demineralized water for about 1 minute.
5. Polishing: 5 minutes "SUBU5", SUBU5 = sulfamic acid (H_3NO_3S , 5 g/l), hydrogen peroxide (H_2O_2 , 5% vol), n-butanol (5% vol) and ammonium citrate (1 g/l) at $72^\circ C$ ($70-75^\circ C$) with bath agitation, 5 samples in a 5L beaker.
6. Pre-rinsing with sulfamic acid (H_3NO_3S , 5 g/l) for about 1 minute, to remove hydrophobic layer.
7. Rinsing with water: demineralized water for about 30 seconds.
8. Spraying with alcohol: ethyl alcohol to enhance drying.
9. Drying with N_2 .
10. Pre-rinsing with sulfamic acid (H_3NO_3S , 5 g/l) for about 1 minute, to remove hydrophobic layer.
11. Rinsing with water: demineralized water for about 1 minute.
12. Spraying with alcohol: ethyl alcohol to enhance drying.
13. Drying with N_2 .
14. Packing in wafer box.

Total average etched thickness = $45,5 \pm 1 \mu m$.

The samples were sent to WP15 partners for the Nb deposition on October 2017.

2.4.2 EP+SUBU Surface Characterization at INFN

Optical Inspection and Reflectivity measure

The substrate presents a **mirror like surface with a diagonal texture** as in the EP case (Figure 10) due to the oxygen evolution during the EP process. The SUBU process reduced the texture, but did not remove it completely.

Reflectivity (400-700 nm): **66 %**.

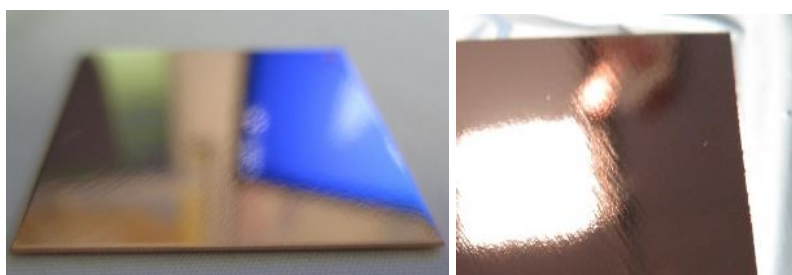


Figure 14 Pictures of a planar sample treated with EP+SUBU process

Roughness

Initial surface (average values on 6 samples), Ra = 130 ± 30 nm

After EP + SUBU (average values on 2 samples), Ra = 115 ± 80 nm

Also in this case the roughness value is strongly influenced by the EP texture. The roughness measured parallel to the texture (blue arrow on Figure 11) is close to the SUBU values.

After EP + SUBU (scan along the diagonal direction), Ra = 59 ± 9 nm

SEM and EDS

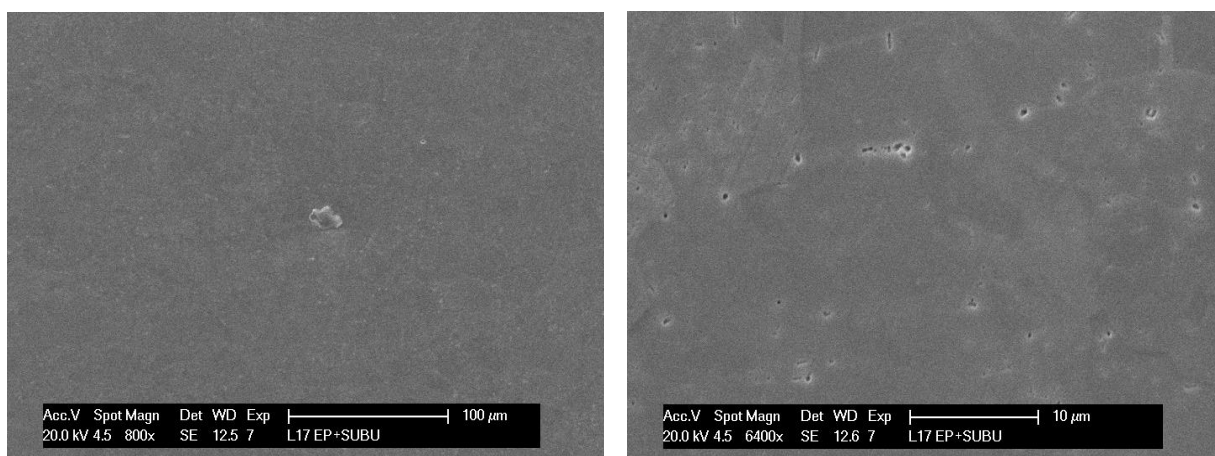


Figure 15 SEM micrographs at two different magnification level of an EP+SUBU treated sample

The SEM characterization shows a very smooth surface. Some pitting is visible, probably caused by the SUBU process.

EDS characterization was also done. After tumbling no visible contaminations appear.

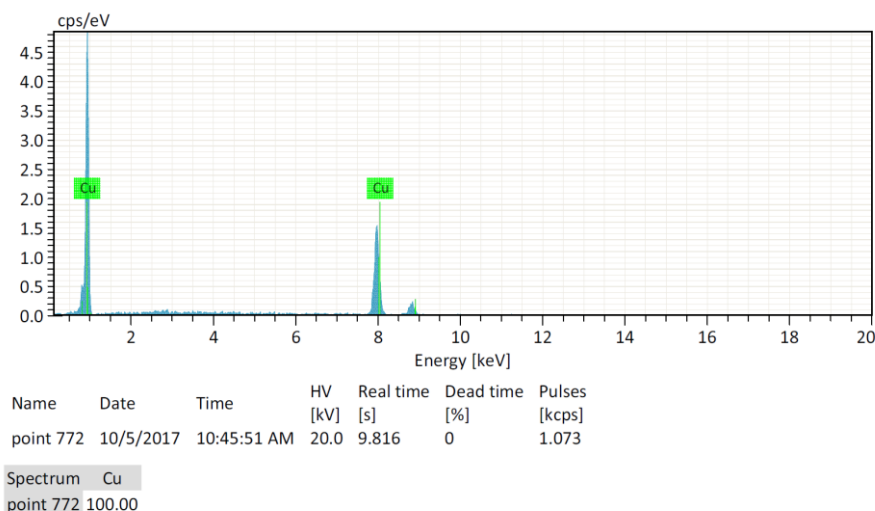


Figure 16 EDS analysis on an EP treated sample

2.5 TUMBLING

Tumbling (also called Centrifugal Barrel Polishing) has been applied to niobium bulk cavities, mostly at KEK and to some extent at DESY [11], and to Nb/Cu cavities at LNL for ALPI QWR [1]. Tumbling effectively removes irregularities like scratches and especially any roughness at electron beam weld seams. Tumbling is also needed for removing the fissures in the initial surface preparation of hydroformed and spun cavities [11].

For the tumbling of ARIES samples a Turbula 3D Powder mixing machine was used. Samples were kept in a sample holder to prevent bending and two different media were used in order to obtain the best results in terms of surface smoothing.

2.5.1 Tumbling Cleaning Procedure at INFN

1. Degreasing: in NGL 1740 bath for about 2 hours, with 3-5 minutes ultra-sonic ON at start and again 3 minutes ultra-sonic ON before end.
2. Polishing: Tumbling with a 3 dimensional motion, in a solution composed by alumina embedded media and Roadastel30 bath.
3. Rinsing with water: demineralized water for about 1 min.
4. Polishing: Tumbling with a 3 dimensional motion using coconut powders as media.
5. Degreasing: in Rodastel bath for about 2 hours, with 3-5 minutes ultra-sonic ON at start and again 3 minutes ultra-sonic ON before end.
6. Pre-rinsing with acid: sulfamic acid ($\text{H}_3\text{NO}_3\text{S}$, 5 g/l) for about 1 minute, to remove hydrophobic layer.
7. Rinsing with water: demineralized water for about 1 minute.
8. Spraying with alcohol: ethyl alcohol to enhance drying.
9. Drying with N_2 .
10. Packing in wafer box.

The etched thickness is controlled by samples weighting.

Due to some problems during the tumbling process, the initial samples were damaged and replaced with new spare samples sent by CERN. The treated samples were sent to WP15 partners for the Nb deposition on March 2018.



Figure 17 Pictures of the Set-up of the tumbling polishing procedure. A) Sample holder, B) Allumina embedded in ureic resin, C) Coconut powders, D) Tumbling barrel filled with alumina media and Rodastel30 bath, E) Tumbling barrel filled with coconut powders, F) Turbula tumbling machine

2.5.2 Tumbling Surface Characterization at INFN

Optical Inspection and Reflectivity measure

The substrate presents a **shining surface** (Figure 18) with small scratches visible only examining the sample from a certain angle. Reflectivity is less compared to SUBU and EP processes.

Reflectivity (400-700 nm): **52 %**.

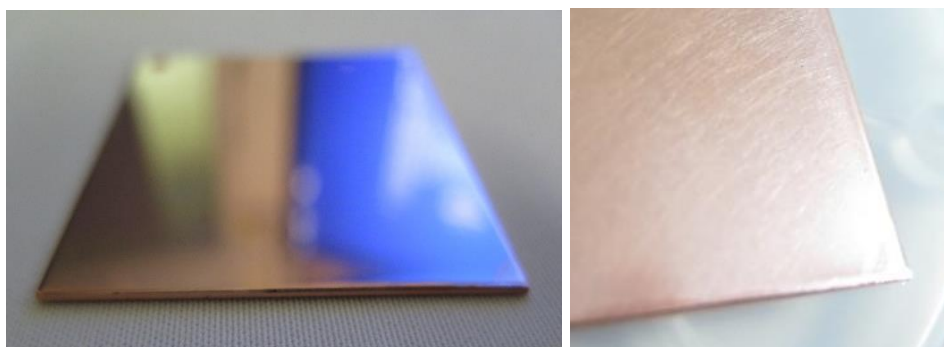


Figure 18 Pictures of a planar sample treated with tumbling process

Roughness

Initial surface (average values on 6 samples), Ra = 130 ± 30 nm

After Tumbling (average values on 2 samples), Ra = 44 ± 7 nm

Roughness is very low, comparable to the SUBU samples one.

SEM and EDS

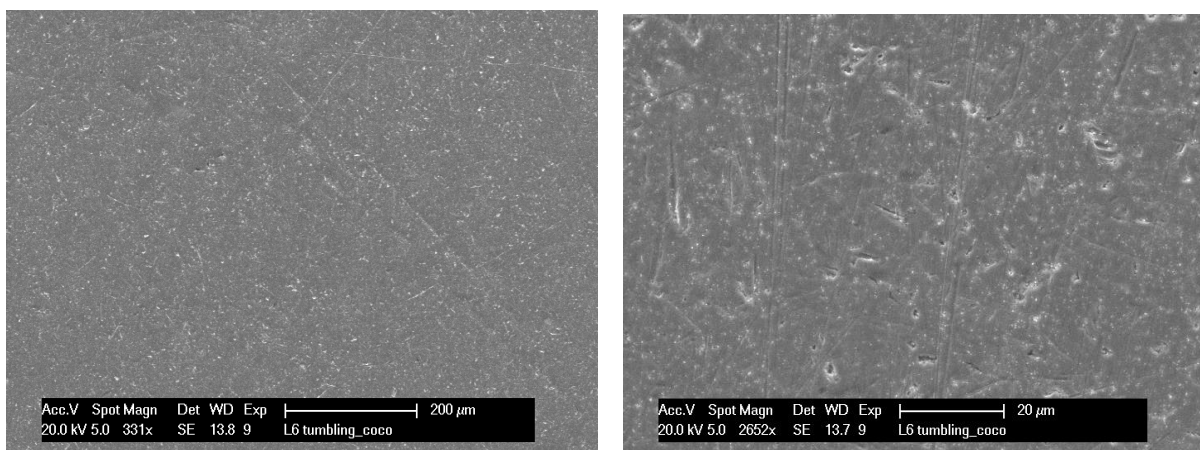


Figure 19 SEM micrographs at two different magnification level of a tumbling treated sample

The SEM characterization shows the presence of a large amount of scratches and defects on the surface. EDS characterization was also done. After EP no visible contaminations appear. A characterization of the section is necessary to evaluate the presence of embedded media material.

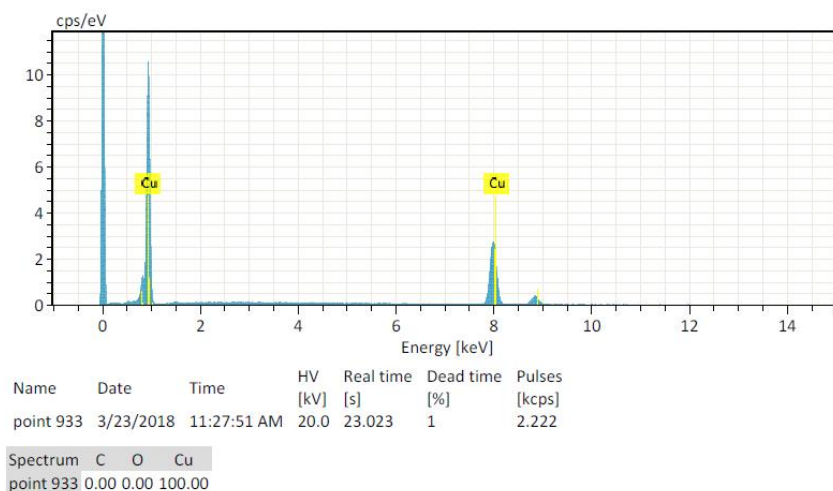


Figure 20 EDS analysis on a tumbling treated sample

2.6 LASER POLISHING AT RTU

Laser Polishing method for Cu surface substrates was studied. For this aim laser cleaning and polishing chamber with inert gas – Argon was constructed (Figure 21). Cu samples, produced by Kurt J. Lesker Company, were irradiated by pulsed nanosecond Nd:YAG laser ($\lambda= 1.064 \mu\text{m}$, $\tau =6 \text{ ns}$ at different intensities in the range of $0.72\text{-}3.28 \text{ GW/cm}^2$) in scanning mode, with $5\mu\text{m}$ step in Ar atmosphere. The intensities of the laser radiation were lower than the ablation threshold of Cu.

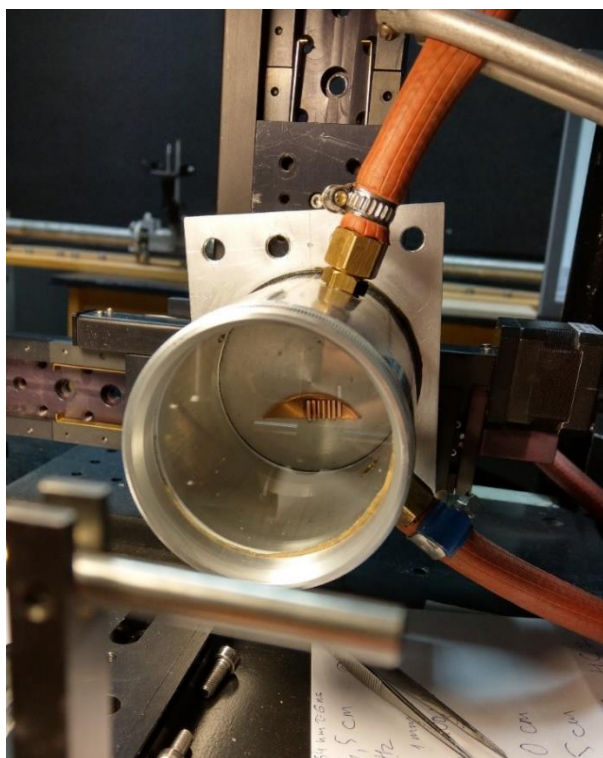


Figure 21 Laser cleaning and polishing chamber with inert gas – Argon

Five areas of the Cu sample were irradiated with different intensities: $I_1= 0.72 \text{ GW/cm}^2$; $I_2= 0.96 \text{ GW/cm}^2$; $I_3=1.46 \text{ GW/cm}^2$; $I_4= 1.89 \text{ GW/cm}^2$; and $I_5=3.28 \text{ GW/cm}^2$. So high values of laser intensity were chosen because of high reflectance of Cu at wavelength $\lambda=1064 \text{ nm}$.

Optical microscope Nikon Eclipse LV150 was used for imaging the surface structure before and after the laser irradiation (Figure 22). The following preliminary results have been obtained: (i) Before irradiation by laser the surface had scratches, which were eliminated when the laser radiation intensity was increased; (ii) At the same time, the studies of 2D AFM images (measured by Veeco Digital Instruments CP-II) of the non-irradiated (Figure 23 top) and the irradiated Cu (Figure 23 bottom) samples and region analysis revealed that the surface roughness RMS (Root Mean Square Roughness) has increased after the irradiation by laser.

Initial results demonstrated that the deep scratched on copper surface can be removed by laser polishing, but the lowest surface roughness obtained was $R_a \sim 200 \text{ nm}$, i.e. much higher than for other techniques. These initial results are promising but more work should be done to make it compatible to other techniques.

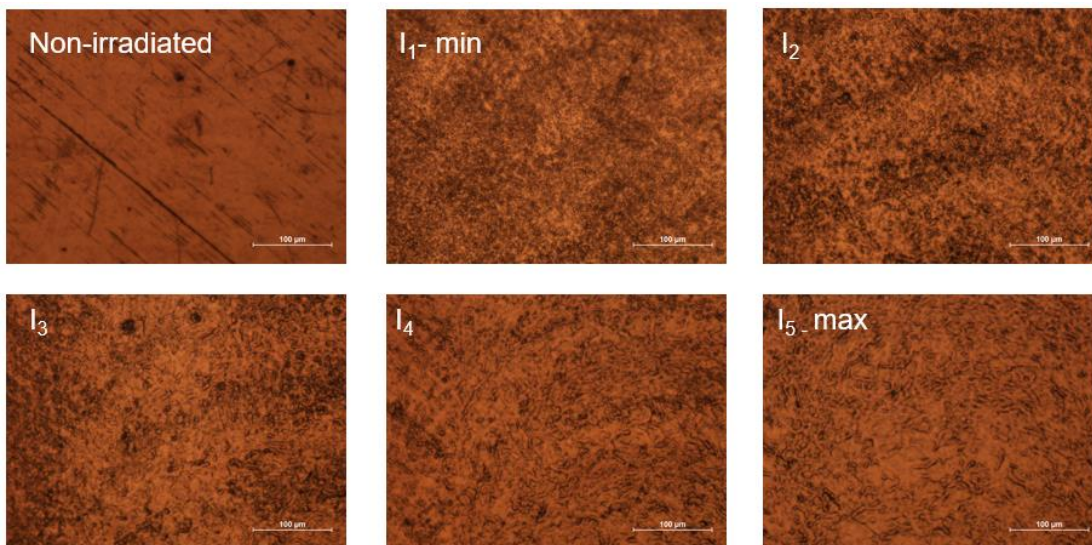


Figure 22 Optical microscope images of non-irradiated and irradiated by nanosecond Nd:YAG laser with different intensities Cu samples from «Kurt J. Lesker Company».

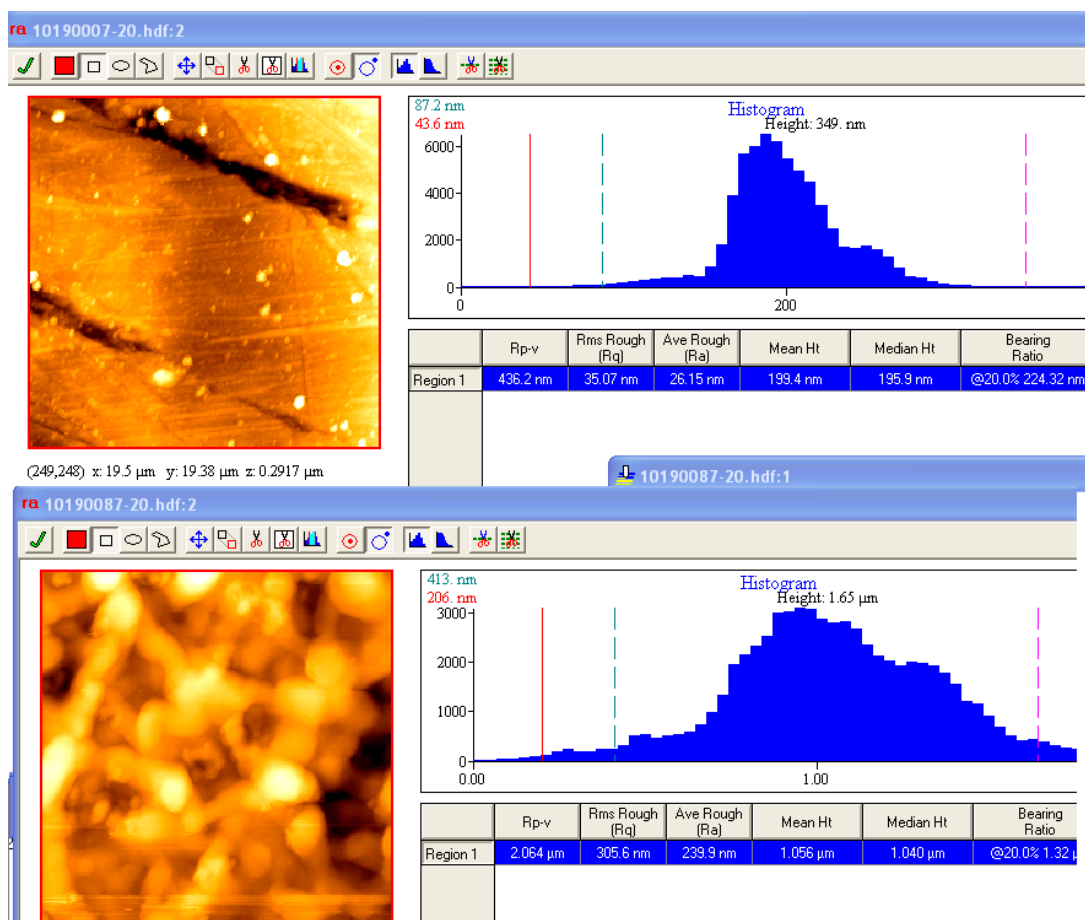


Figure 23 AFM images of sample from «Kurt J. Lesker Company»: Non-irradiated (top) and irradiated by nanosecond Nd:YAG laser radiation with intensity $I_1 = 0.723 \text{ GW/cm}^2$ (bottom).

2.7 SURFACE CHARACTERIZATION COMPARISON

Table 1 Roughness comparison between the 4 polishing treatments evaluated

Polishing Treatment	Ra	Ra diagonal
<i>Initial surface</i>	$130 \pm 30 \text{ nm}$	
SUBU5	$48 \pm 7 \text{ nm}$	
EP	$225 \pm 80 \text{ nm}$	$86 \pm 14 \text{ nm}$
EP+SUBU5	$115 \pm 80 \text{ nm}$	$59 \pm 9 \text{ nm}$
Tumbling	$44 \pm 7 \text{ nm}$	

Table 2 Reflectivity comparison between the 4 polishing treatments evaluated

Polishing Treatment	Ra
SUBU5	65 %
EP	64 %
EP+SUBU5	66 %
Tumbling	52 %

Table 3 Surface aspect comparison between the 4 polishing treatments evaluated (visual inspection)

Polishing Treatment	Surface defects
<i>Initial surface</i>	<i>Roll forming texture</i>
SUBU5	Mirror like surface
EP	Mirror like surface with a texture
EP+SUBU5	Mirror like surface with a texture
Tumbling	Shining surface with small scratches visible only examining the sample from a certain angle

Table 4 Surface defects comparison between the 4 polish treatments evaluated (SEM analysis)

Polishing Treatment	Surface defects
<i>Initial surface</i>	<i>Roll forming texture</i>
SUBU5	Pitting
EP	No defects visible
EP+SUBU5	Pitting (less than SUBU5 surface)
Tumbling	Scratches

3. Nb film deposition (task 15.3)

The task of deposition was pursued by STFC, INFN and University of Siegen. For the first set of depositions it was decided to use a deposition method that is available at all three centres. Therefore planar DC magnetron was chosen. Although the deposition configuration is different from one centre to another, the deposition parameters were set to be comparable.

The procedure and the applied deposition parameters in all three deposition facilities are shown in Table 5.

The agreed film thickness was 3 μm .

After deposition with Nb film the original samples with a size of 53 mm x 53 mm were cut as shown in the layout in Figure 24. The pieces were send to WP partners for different characterisation facilities:

- Surface and film characterisation for film composition and morphology to be characterised in the depositing laboratory;
- Laser treatments and film adhesion in RTU
- Film characterisation with thermal electron and exoelectron emission in RTU;
- Superconductivity evaluation at IEE.

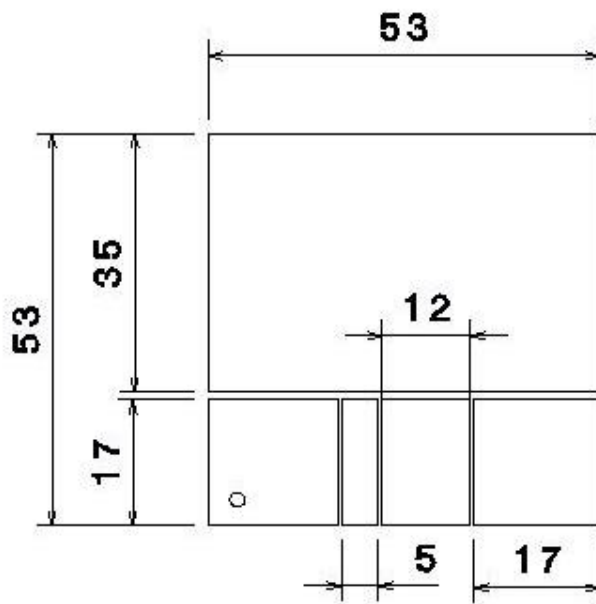


Figure 24 On the left the cutting scheme of the coated samples. Sample dimensions before coating 53 x 53 mm².
On the right Samples cutting set-up at INFN.

Table 5: Parameters set for the synthesis of Nb thin films on Cu using DC magnetron sputtering.

Parameter	STFC	Uni Siegen	INFN
Substrate heated	650 °C for 12 h	650 °C for 1.25 h	650° for >40 h
Base pressure @ 650 °C on a substrate	<10 ⁻⁹ mbar	1.22x10 ⁻⁵ mbar	< 9x10 ⁻⁸ mbar
Deposition temperature	650 °C	650 °C	650 °C
Power supply	DC MS	DC MS	DC MS
Current	0.97A	1.34 A	2.1 A
Current density	22 mA/cm ²	15 mA/cm ²	27 mA/cm ²
Voltage	411V	298 V	≈ 350 V
Target power	400 W	400 W	≈ 750 W
Discharge gas	Kr	Ar	Ar
Discharge gas pressure	1.5x10 ⁻³ mbar	1.5x10 ⁻² mbar	5x10 ⁻³ mbar
Target-substrate distance	10 cm	6 cm	10 cm
Substrate rotation	4 rpm	n/a	no
Deposition time	480 min	20 min	20 min
Deposition rate	7 nm/min	150 nm/min	150 nm/min

3.1 SAMPLE DEPOSITION AT STFC

Samples C7, L13, L18, L19, and L4 have been coated with a 3 μm thick Nb film. Succeeding the deposition, the samples have been cut into pieces and sent to project partners for characterization. The procedure for film deposition using the parameters tabulated in Table 5 was as follow:

1. Unpacking of Sample and directly installing it onto the sample holder.
2. Substrate plate was placed into the load lock (total of five) and load lock evacuated.
3. Deposition chamber and the load lock was baked at 150 C for three days and base pressure of 2x10⁻¹⁰ mbar was achieved.
4. The sample plate was loaded into the deposition chamber and the sample was heated at 650 °C for 12 hours.
5. Kr gas was introduced into the chamber and at the same time the pumping speed reduced via butterfly valve.
6. Target was sputtered cleaned for 5 min.
7. Substrate was deposited without any interruption for 8 hours.
8. Cool down over night.
9. Sample transferred to load lock and new sample was placed in deposition position.
10. Samples were taken out of the load lock once all the samples were deposited.
11. Cutting the samples according to the sketch shown in Figure 24. Using a table top cut-off machine for the 17 mm strip and a small, automatic table top precision cut-off machine for the sectioning of the strip.

12. Rinsing the pieces in ethanol then in distilled water and dry-blow.
13. Packing in membrane film boxes for shipping.

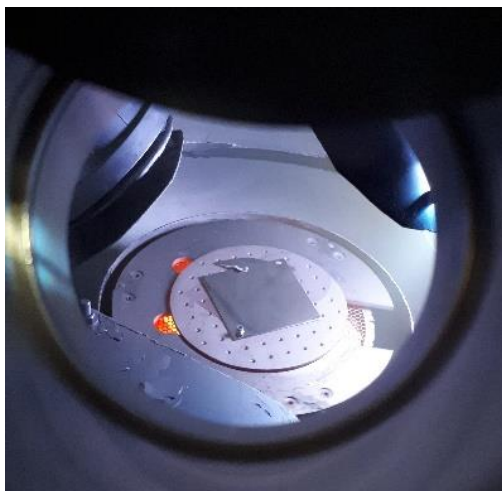


Figure 25 Copper substrate during Nb deposition at STFC

3.1.1 STFC Nb film Surface Characterization

At STFC the following surface characterizations are planned on the coated samples:

1. SEM – Plain view and cross-sectional view
2. EDS
3. XRD
4. XPS

At the moment SEM micrographs on samples C7, L13, L18 and L19 were done.

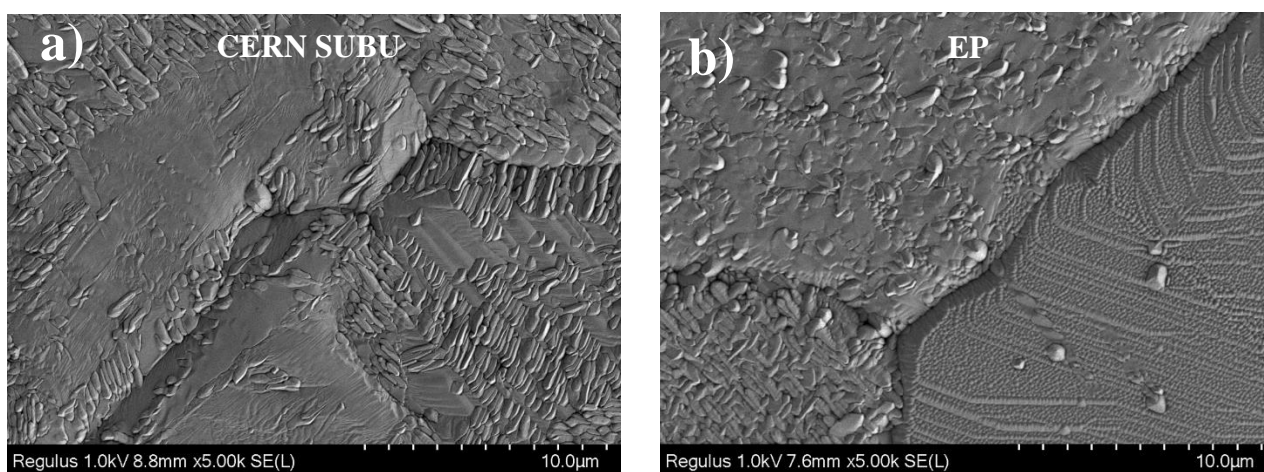


Figure 26 SEM micrographs of the coated sample surface (plan view). a) C7 (SUBU CERN, deposited with Nb at STFC), b) L13 (EP, deposited with Nb at STFC)

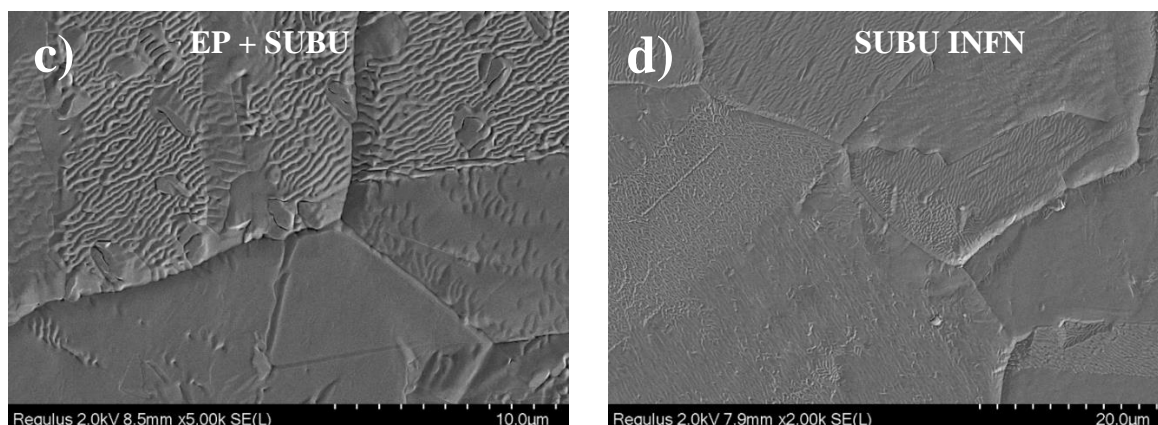


Figure 27 SEM micrographs of the coated sample surface (plan view) c) L18 (EP+SUBU, deposited with Nb at STFC), d) L19 (SUBU INFN, deposited with Nb at STFC)

3.2 SAMPLE DEPOSITION AT SIEGEN

Samples C1, L1, L9, L10, and L23 have been coated with a 3 µm thick Nb film. Succeeding the deposition, the samples have been cut into pieces and sent to project partners for characterization. The below listed procedure and deposition parameters of Table 5 have been applied:

1. Unpacking of Sample and directly installing it onto the sample holder.
2. Chamber evacuation and baking at 650 °C for 1.25 h
3. Subsequent deposition without interruption of the process
4. Cooldown
5. Opening the chamber and packing the sample into its original storage box
6. Cutting the samples according to the sketch shown in Figure 24 using a tabletop cut-off machine for the 17 mm strip and a small, automatic tabletop precision cut-off machine for the sectioning of the strip.
7. Rinsing the pieces in ethanol then in distilled water and dry-blow.
8. Packing in membrane film boxes for shipping.



Figure 28 Open deposition chamber with Nb target (right) and installed Cu substrate (left).

3.2.1 Siegen Nb film Surface Characterization

Table 6: Summary of AFM measurements performed on three different spots of the Nb coated sample. Ra value is the average of three measurements.

Sample name	Substrate treatment	AFM - Roughness (Ra) [nm]
C1	SUBU CERN	21 ± 12.1
L1	SUBU INFN	6.3 ± 1.2
L9	Tumbling	18.3 ± 1.5
L10	EP	11.5 ± 0.7
L23	EP + SUBU	14.2 ± 2.4

AFM measurements were performed in non-contact mode. Scan area was 5 x 5 μm. Three successive scans on different sample spots were taken. Figure 29 shows one example measurement for each sample.

The scans show a high deviation of roughness on the three measured spots in case of sample C1. Consequently, the measurements should be correlated with SEM surface micrographs because the AFM scan maps a very small fraction of the overall sample surface only. Figure 30 shows SEM investigations of all five samples. It becomes obvious that on the SUBU samples two different grain structures can be observed. That is, areas with lower grain size and lower roughness, and areas with higher grain size and, therefore, higher surface roughness. The findings correlate with the SEM investigations of the uncoated substrate: it is shown that the SUBU pretreatment leads to anisotropic etching of the different grain orientations on the polycrystalline Cu substrate. This, in turn, leads to different growth mechanisms of the deposited film. Another phenomenon of the SUBU treatment revealed by the SEM investigations is pitting which leads to areas with very high roughness values and high deviation of these values. The EP, by contrast, shows less deviation of Ra which also correlates with the SEM investigation. The lowest roughness values are measured on SUBU samples provided by INFN (L1). This is in contrast with the before mentioned findings. However, the inspected area by AFM is small. If the measurement does not cover one of the areas showing high roughness due to the above-mentioned effect, the result is reasonable.

The morphology of the coating itself is typical for a fine columnar growth, showing the tips of the columns with diameters in the range of some tenth of nanometers up to 100 nm in both, AFM and SEM investigations.

All coatings show a considerable amount of oxygen, revealed by EDX measurements. Figure 32 shows the EDX measurement of sample L1 which represents all remaining films. The existence of Oxygen can be correlated with the very small and columnar grains. The unwanted Oxygen content in the coatings is caused by the relatively high base pressure of the vacuum system of 1.22×10^{-5} mbar. Latest tests show that the system's base pressure can attain an ultimate pressure $< 5 \times 10^{-7}$ mbar which will be applied in the future coatings.

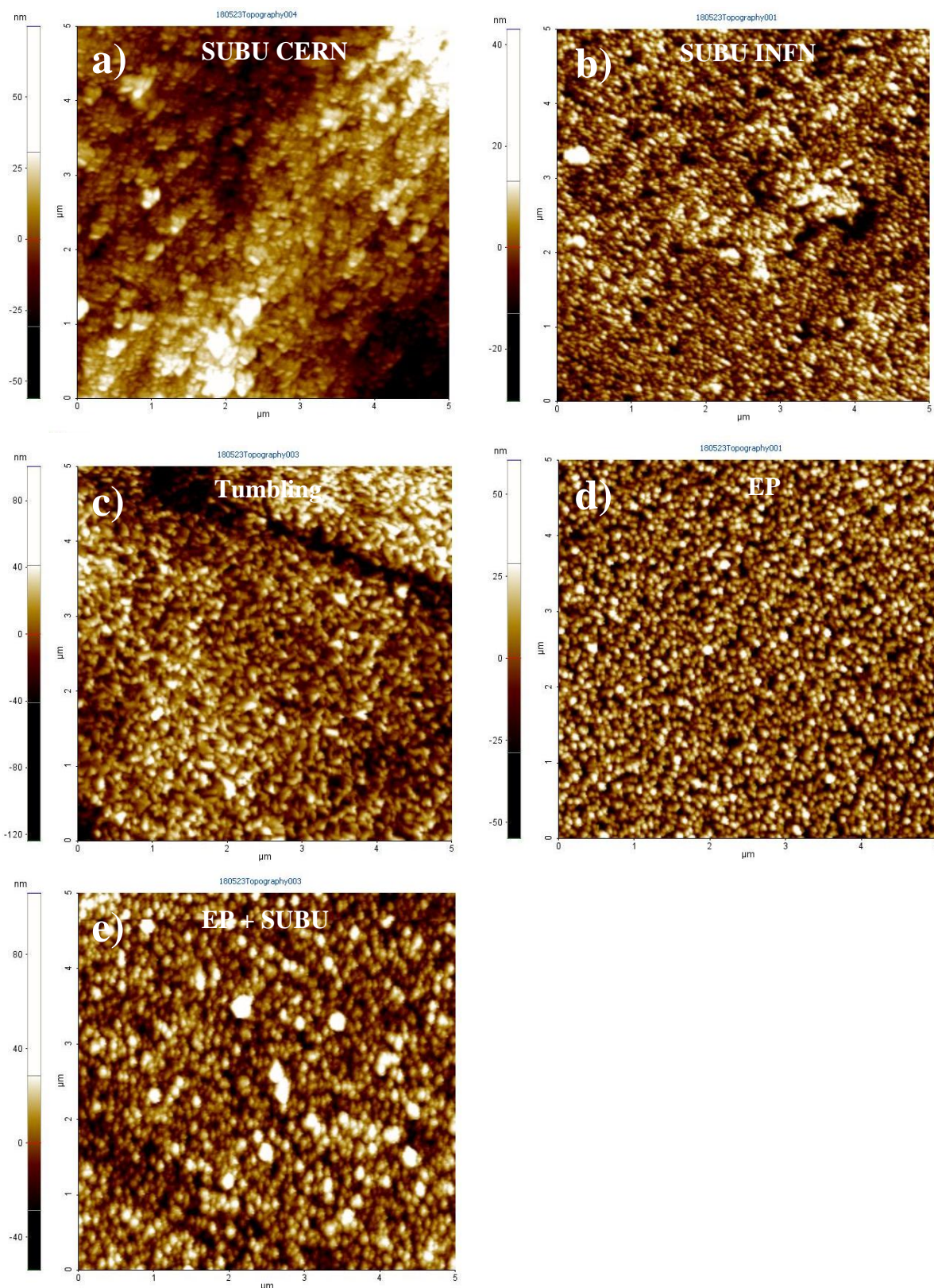


Figure 29: AFM measurements of samples deposited with Nb at UniSiegen a) C1, b) L1, c) L9, d) L10, and e) L23.

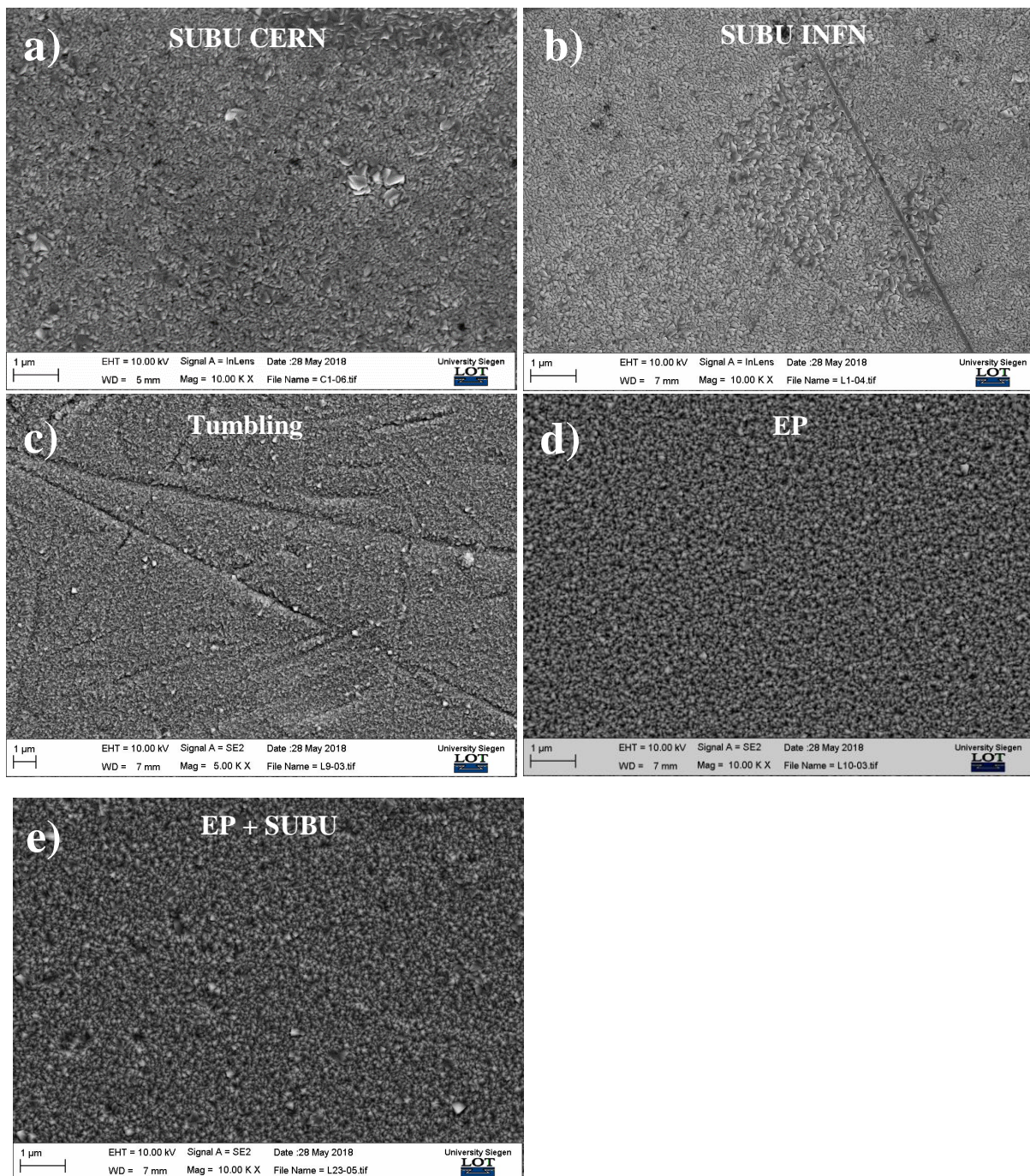


Figure 30: SEM micrographs of the coated sample surface (plan view). All samples deposited with Nb at UniSiegen.
 a) C1 (SUBU CERN), b) L1 (SUBU INFN), c) L9 (Tumbling), d) L10 (EP), e) L23 (EP+SUBU)

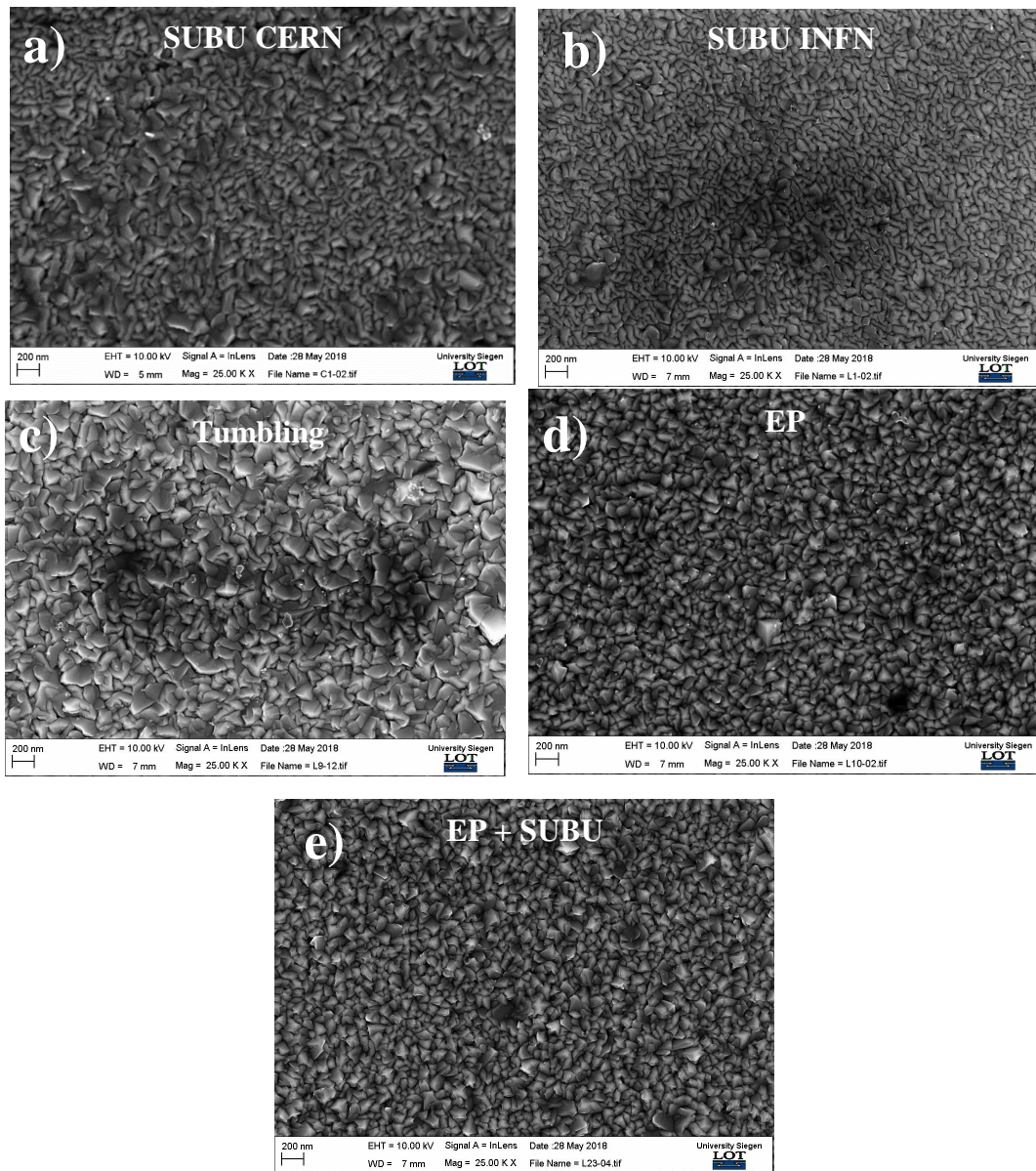


Figure 31: Same SEM micrographs as in Figure 30 but higher magnification.

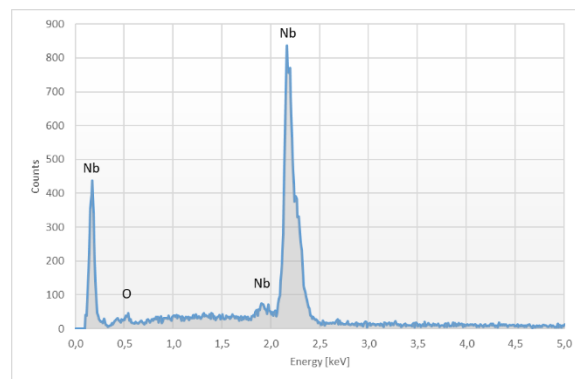


Figure 32: EDX of Sample L1 (sample deposited with Nb at UniSiegen), representing all other samples.

3.3 SAMPLE DEPOSITION AT INFN

Samples C10, L8, L16, L20, and L21 have been coated with a 3 μm thick Nb film. Succeeding the deposition, the samples have been cut into pieces and sent to project partners for characterization. The below listed procedure and deposition parameters of Table 5 have been applied:

1. Unpacking of Sample and directly installing it onto the sample holder.
2. Chamber evacuation and baking at 650 °C for more than 40 hours.
3. Target conditioning for 5 minutes.
4. Subsequent deposition without interruption of the process for 20 min.
5. Cooldown for more than 15 hours.
6. Opening the chamber and packing the sample into its original storage box.
7. Cutting the samples according to the sketch shown in Figure 24.
8. Rinsing the pieces in ethanol and dry with nitrogen.
9. Packing in PE bags and millipore boxes for shipping.

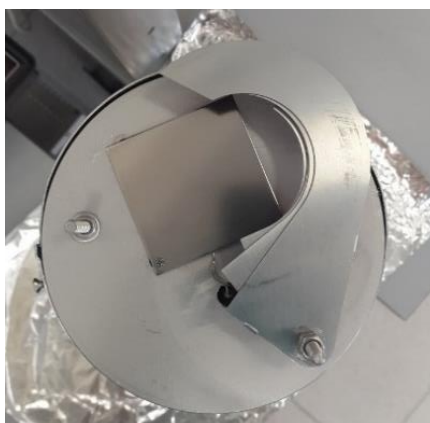


Figure 33 Copper substrate after Nb deposition at LNL

3.3.1 INFN Nb film Surface Characterization

On the five samples coated at INFN 4 different characterizations were done:

- a) Roughness
- b) SEM
- c) EDS
- d) XRD

Roughness

The roughness was measured with a profilometer Veeco Dektat 8, using the same parameters used for Polished sample (see paragraph 0).

Scan length: 1 mm, applied force 12 mg. 3 scan on 2 different direction (a total of 6 scan) has been done in order to take into account the roll forming texture.

Table 7 Roughness comparison between the five coated samples

Sample	Ra	Ra diagonal
SUBU5 CERN (C10)	126 ± 15 nm	
SUBU5 INFN (L20)	197 ± 98 nm	
EP (L21)	233 ± 66 nm	254 ± 50 nm
EP+SUBU5 (L16)	192 ± 64 nm	96 ± 18 nm
Tumbling (L8)	207 ± 53 nm	

Data dispersion is very high and all samples present similar roughness. Probably, the roughness values are strongly influenced by the sample bending due to cutting. On the other hand this could be due to faceting during the growth of the Nb film.

SEM and EDS

A Philips XL 30 as SEM and a Bruker X-Lash Detector 410-M for the EDS analysis have been used. The Nb surface reproduced the original one as was expected. On SUBU and EP+SUBU pitting is visible, on the tumbling sample scratches are reproduced by the Nb morphology. EP surface shows the grain boundary of the Nb film.

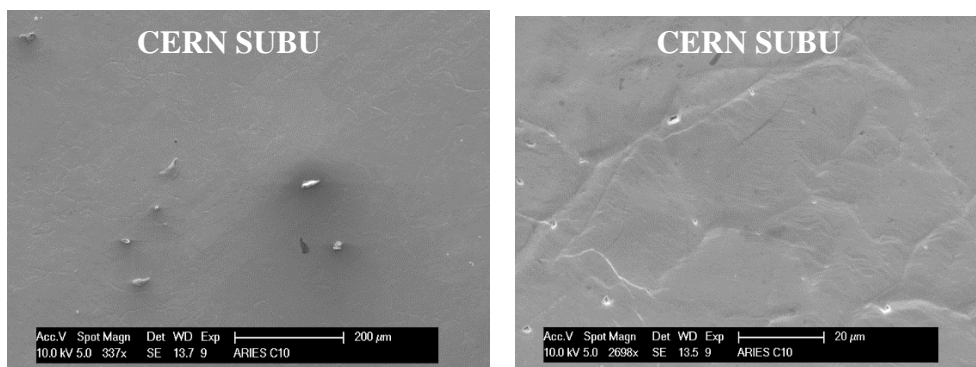


Figure 34 SEM micrographs at two different magnification level of Nb coating on a CERN SUBU5 treated sample (C10 sample deposited at INFN)

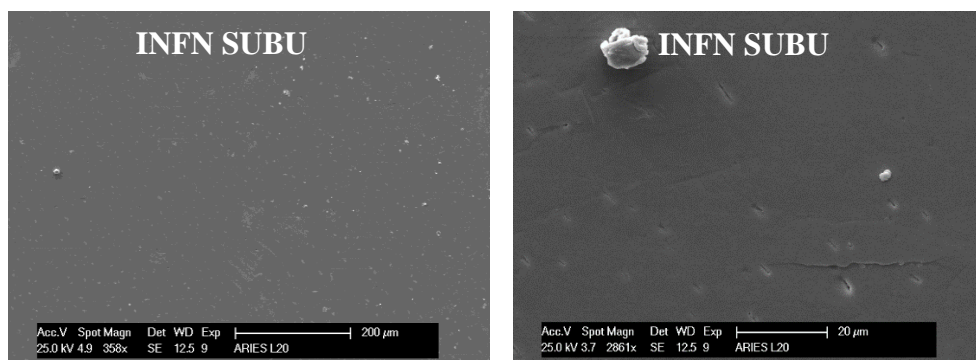


Figure 35 SEM micrographs at two different magnification level of the Nb coating on a INFN SUBU5 treated sample (L20 sample deposited at INFN)

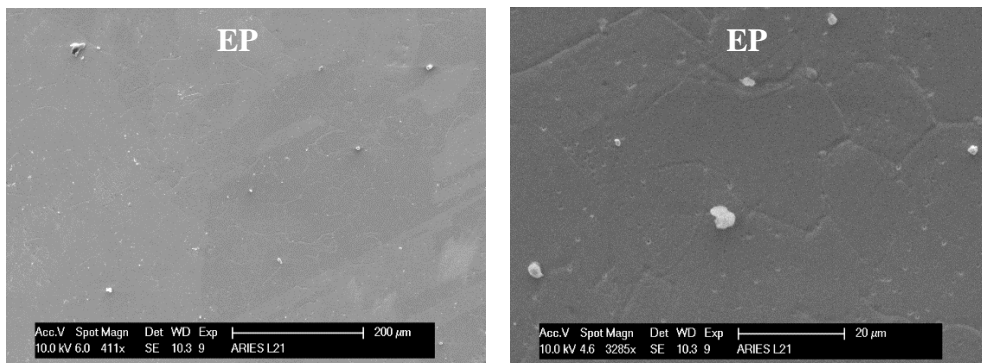


Figure 36 SEM micrographs at two different magnification level of the Nb coating on a EP treated sample (L21, sample deposited at INFN)

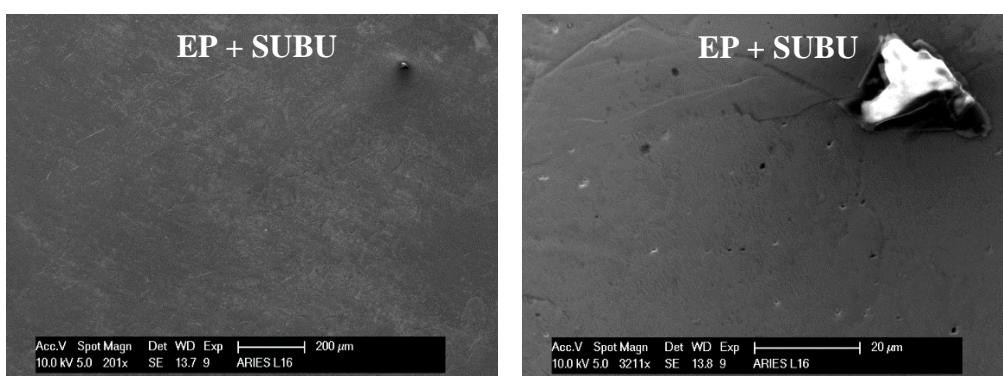


Figure 37 SEM micrographs at two different magnification level of the Nb coating on a EP+SUBU treated sample (L16 sample deposited at INFN)

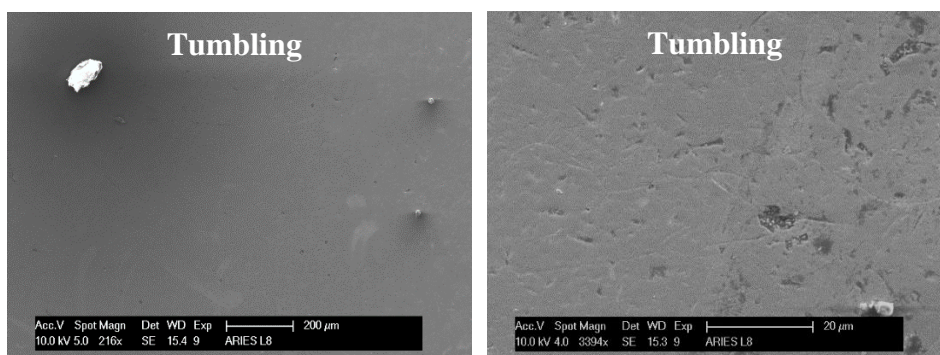


Figure 38 SEM micrographs at two different magnification level of the Nb coating on a Tumbling treated sample (L8 sample deposited at INFN)

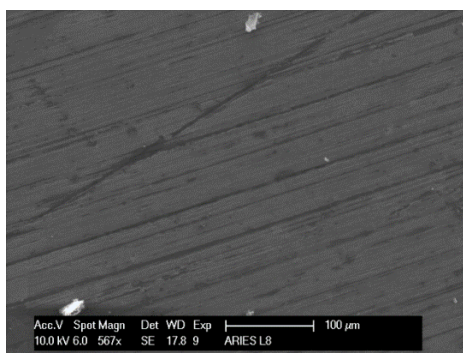


Figure 39 SEM micrograph of the Nb coating on a Tumbling treated sample (L8), near the sample hole. The screw prevents the sample from tumbling polishing and the film growth replicate the roll forming texture of the untreated sample.

EDS characterization was also done. No visible contaminations appear in analysed samples.

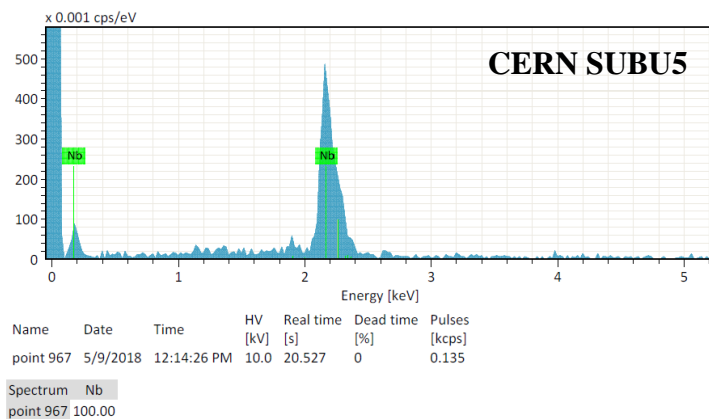


Figure 40 EDS analysis on Nb coating of a CERN SUBU5 treated sample (C10)

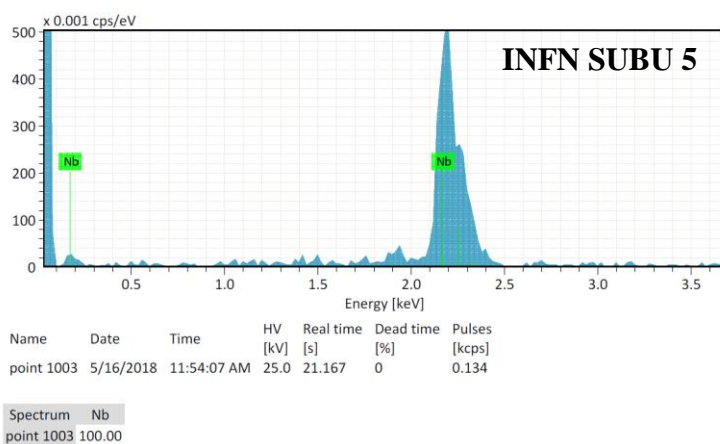


Figure 41 EDS analysis on Nb coating of a INFN SUBU5 treated sample (L20 sample deposited at INFN)

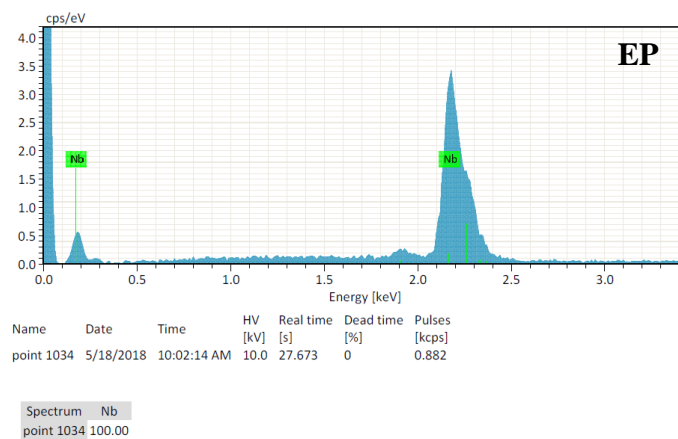


Figure 42 EDS analysis on Nb coating of a EP treated sample (L21 sample deposited at INFN)

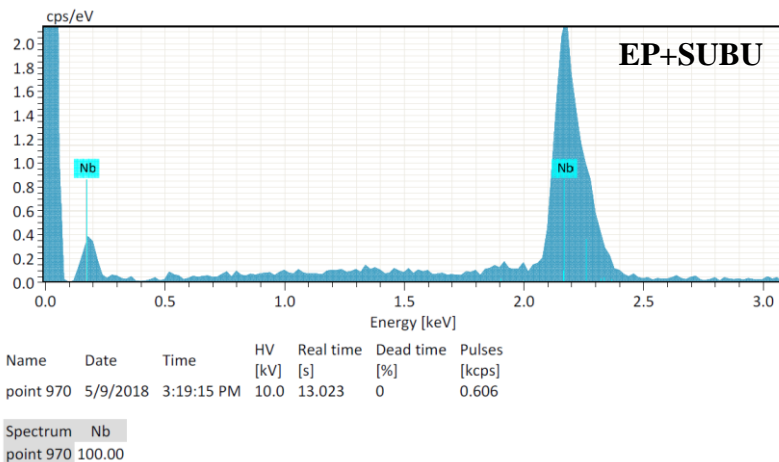


Figure 43 EDS analysis on Nb coating of a EP+SUBU treated sample (L16 sample deposited at INFN)

XRD

The crystal structure of Nb films was characterized by monochromatic Cu-K α radiation on a Philips X'Pert X-ray diffractometer operated at 40 kV and 40 mA.

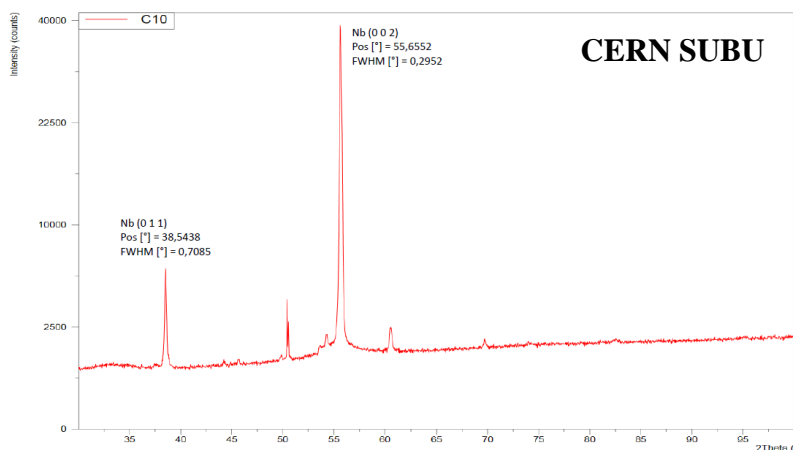


Figure 44 XRD analysis on Nb coating of a CERN SUBU5 treated sample (C10 sample deposited at INFN)

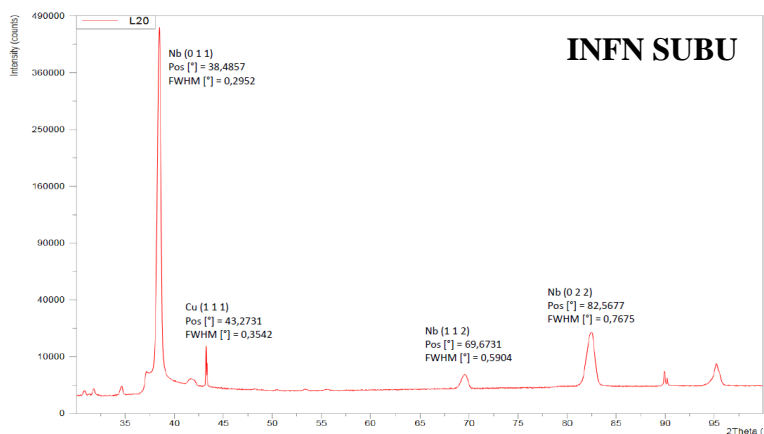


Figure 45 XRD analysis on Nb coating of a LNL SUBU5 treated sample (L20 sample deposited at INFN)

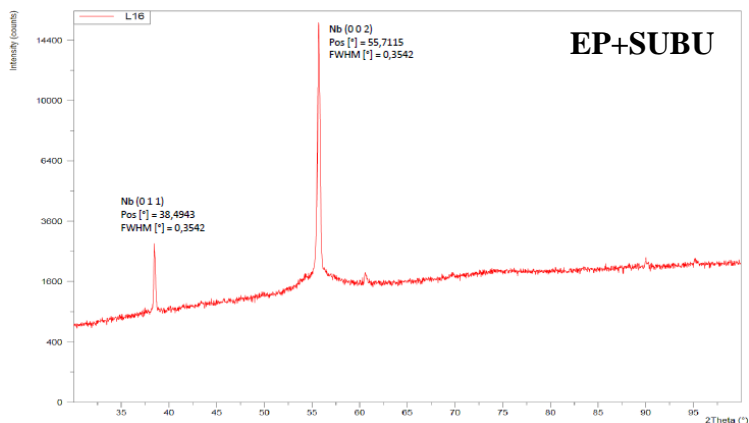


Figure 46 XRD analysis on Nb coating of a EP+SUBU treated sample (L16 sample deposited at INFN)

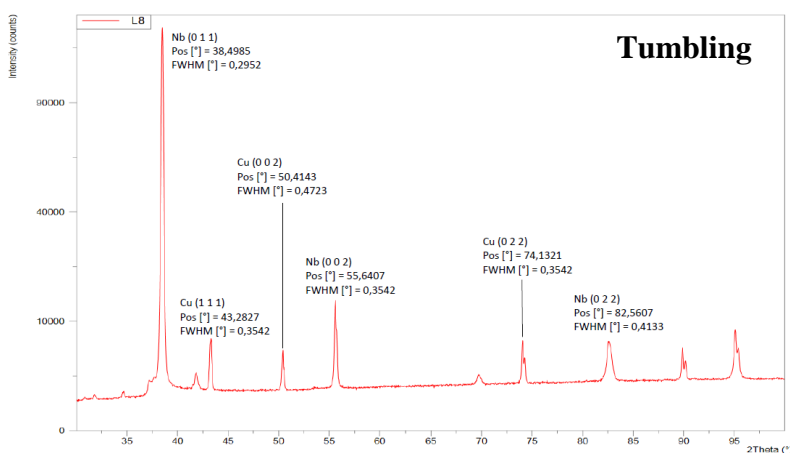


Figure 47 XRD analysis on Nb coating of a Tumbling treated sample (L8 sample deposited at INFN)

3.4 FILM CHARACTERISATION WITH THERMAL ELECTRON AND EXOELECTRON EMISSION AT RTU

Goal

Exploration of the **thermostimulated exoelectron emission (TSE)** and **photothermostimulated exoelectron emission (PTSE)** of the Nb films, deposited on the substrates, initially pre-processed by different methods. Differences in TSE and PTSE spectra (glow curves) could indicate differences in the structure / concentration of defects of the deposited films.

Capacity

Thermostimulated and photothermostimulated exoelectron spectroscopy indicates that heat induced structural relaxations of the surface layer (the electrons emit from the depth 10-100 nm), however, this emission is induced because of the structural transformations (annealing of the structural defects, their migration to the surface) that could be developed at the μm scale.

Measurement procedure

TSEE and PTSEE were measured for the specimens C10, L8, L16 and L20. Specimen was heated in vacuum from 20°C up to 510°C at the rate 10°C/s. During heating, specimen was from time to time (every 10 °C) illuminated by narrow light beam with wavelength 250 nm (beam area < 0.5×2 mm). The emitted electron flux I (particles·s⁻¹) was measured by secondary electron multiplier detector. By this way, both thermostimulated (TSE) and photothermostimulated (PTSE) exoelectron emission were measured.

Results

PTSE and TSEE spectra of Nb on CU specimens are presented at Figure 48. All spectra were normalised on maximum electron flux, averaged at the maximum, so that sharp bursts of emission are excluded. PTSE spectra of all specimens demonstrated two maxima that could correspond to annealing of two type of structural imperfections. For the specimen L8, only rising branch of the 2nd maximum is revealed. As a first approach, annealing curve could be described by Randal-Wilkins expression, widely used for description of thermoluminescence glow curves. This expression use three parameters: activation energy E , frequency factor S and number / concentration of imperfections N_0 . Since one has used normalised PTSE and TSEE data, the concentration N_0 and frequency factor S should be interpreted just as matching parameter. E , in turn, is specific for the particular imperfection. Application of Randal-Wilkins expression to the PTSE curves (Figure 49) allows to roughly evaluate parameters E and S for PTSE peaks. For the high – temperature peak, the Randal-Wilkins curve was matched with the rising branch of the peak only.

TSEE spectra of all specimens demonstrated high – temperature peaks, whose maximum's temperature coincides generally with PTSE maxima. The low temperature peak is observed for L8 and C10, but is negligible for L16 and L20. From the other hand, L16 and L20 demonstrates sharp emission bursts at ~465°C (L16) and 420°C, 475°C and 500°C (L20). The nature of such bursts is not clear, but appearance of such bursts at the PTSE spectra of L20 at 420°C, could indicate that the bursts are related to some fast relaxation process in Nb film.

The activation energy of the low - temperature peaks for the specimens L8 and C10 was lower, comparing to ones of L16 and L20. As compared t other specimens, L16 showed higher activation energy for high - temperature peak, but L20 – for the low temperature peak.

The interpretation of obtained data required additional research to understand underlying physical process, Although alterations of relative intensity, activation energy and positions of the peaks indicates that structure / nature of imperfections in the Nb film is changed due to different pre-processing of the Cu substrate.

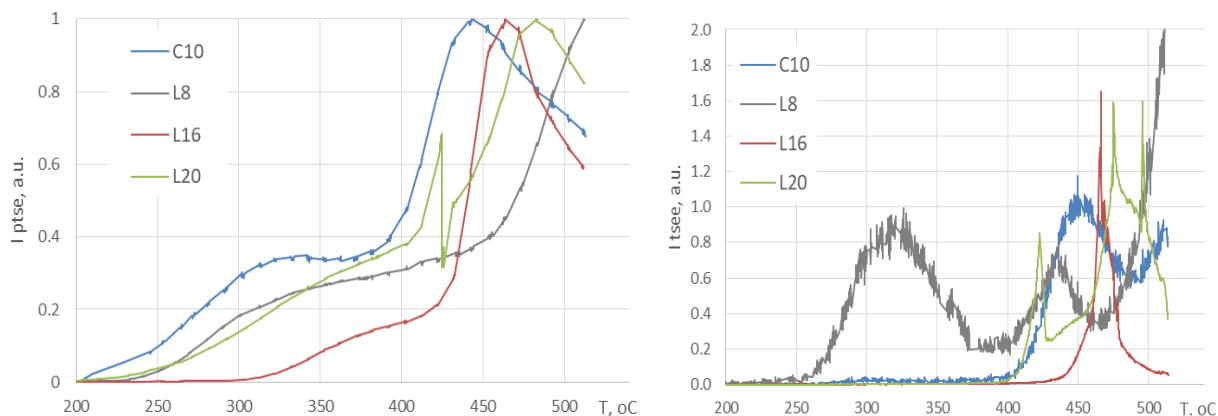


Figure 48 PTSE (left) and TSEE (right) spectra of Nb film on Cu

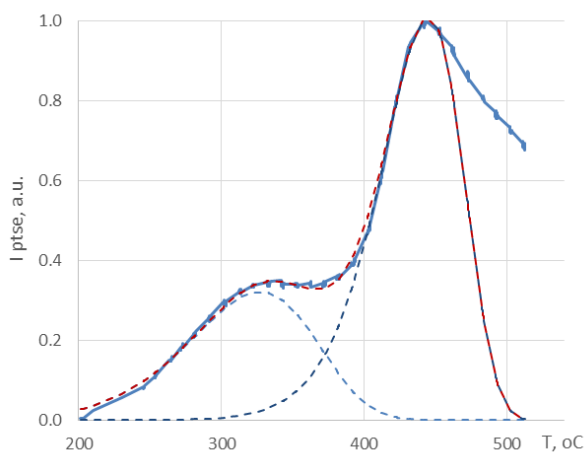


Figure 49 Approximation of PTSE spectrum of the using Randal-Wilkins model

Table 8 Parameters of TSEE / PTSE spectra of Nb – on – Cu specimens

Specimen	PTSE				TSEE	
	Low-temperature peak		High-temperature peak		Low-T peak	High-T peak
	E, eV	T _{max} , °C	E, eV	T _{max} , °C	T _{max} , °C	T _{max} , °C
C10	320	0.65	450	1.50	310	450
L8	362	0.56	> 500	1.42	320	425
L16	375	1.26	460	2.48	-	470
L20	370	1.82	490	1.75	425	490

4. SC properties evaluation at IEE (task 15.4)

Flat samples of approximately 12 x 17 mm with Nb layer deposited on one side of 1 mm thick Cu substrate were received from partners for characterization of superconducting parameters.

In the first step we have measured virgin DC magnetization curves on small measurement samples, approximately 2 x 2 mm, cut from the as-received ‘master’ samples with the help of laboratory cut-off machine (saw) with a SiC cut-off disc. The magnetization curves were measured on samples cooled down below T_c in zero applied magnetic field (zero-field-cooled conditions, ZFC). The external magnetic field was applied perpendicular to the flat face of the samples. The critical temperature was determined in AC susceptibility measurements as the onset of the real part decrease from constant (zero) level with decreasing temperature, at constant AC magnetic field amplitude (0.1 mT) and zero DC magnetic field applied to the sample. The T_c values for all the investigated samples lie between 9.2 K and 9.7 K.

Following characteristic fields were determined from the virgin magnetization curves:

- B_{en} – applied field at which the magnetic flux starts entering the sample’s volume. It was detected as the field at which the virgin magnetization curve starts to deviate from the linear dependence, which the virgin curve follows in the initial part starting from the zero applied field. The field B_{en} was determined employing 2% relative difference criterion, i.e. as the applied field at which the relative difference between the virgin magnetization curve and the initial linear trend reaches 2%. B_{en} is proportional to the first (lower) critical field B_{c1} through a geometrical constant that depends on the dimensions of the sample. The linear fit of the initial, low-field part of the virgin magnetization curve of the form $m_M = \alpha B + \beta$ (α, β – constants) was also used to normalize the data.
- B_p – applied field at which the minimum (maximum moment in absolute value) of the virgin magnetization curve is reached. It is proportional to the full penetration field of the sample via a geometrical constant given by the sample dimensions.
- B_{c2} – Second (upper) critical field, estimated as the applied magnetic field at which the virgin magnetization curve reaches the constant dependence at almost-zero magnetic moment in the region of high fields.

The results and B_{en} , B_p , B_{c2} values determined for the individual samples are summarized in following graphs, ‘Bdc’ denotes the applied homogenous magnetic field and ‘m’ the measured magnetic moment in all of them.

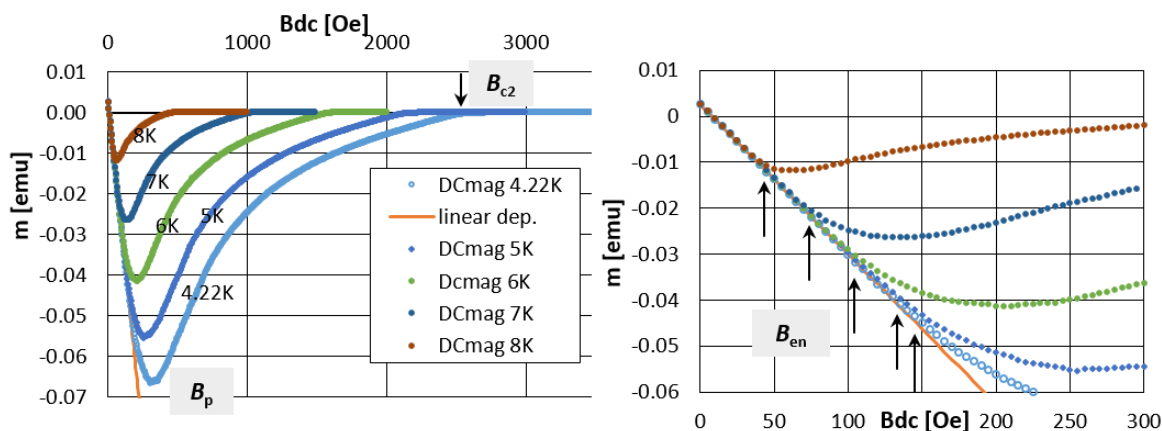


Figure 50 Illustration of the characteristic fields B_{en} , B_p , B_{c2} . Experimental curves of sample L16 are used as an example. The orange line shows the linear fit to the initial part of the curves mM . [$1 \text{ Oe} = 0.1 \text{ mT}$ (in vacuum), $1 \text{ emu} = 10^{-3} \text{ Am}^2$]

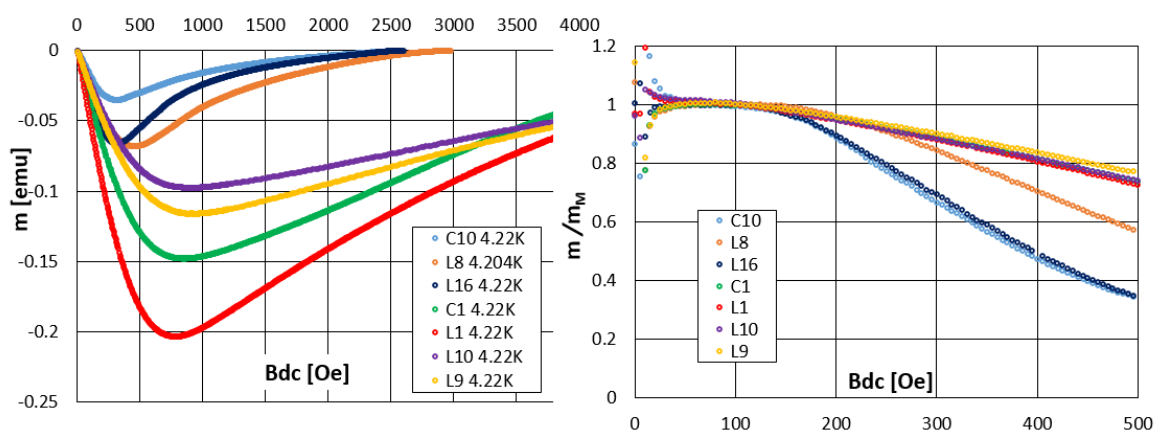


Figure 51 Virgin magnetization curves measured at 4.22 K for all the investigated samples (left) and the same curves normalized with the initial linear (“Meissner”) dependences mM (right). The data scatter observed at the very lowest applied fields is caused by a small residual external field present in the extraction magnetometer set-up during the sample cool-down, i.e. not following absolutely precisely the ZFC conditions. [$1 \text{ Oe} = 0.1 \text{ mT}$ (in vacuum), $1 \text{ emu} = 10^{-3} \text{ Am}^2$]

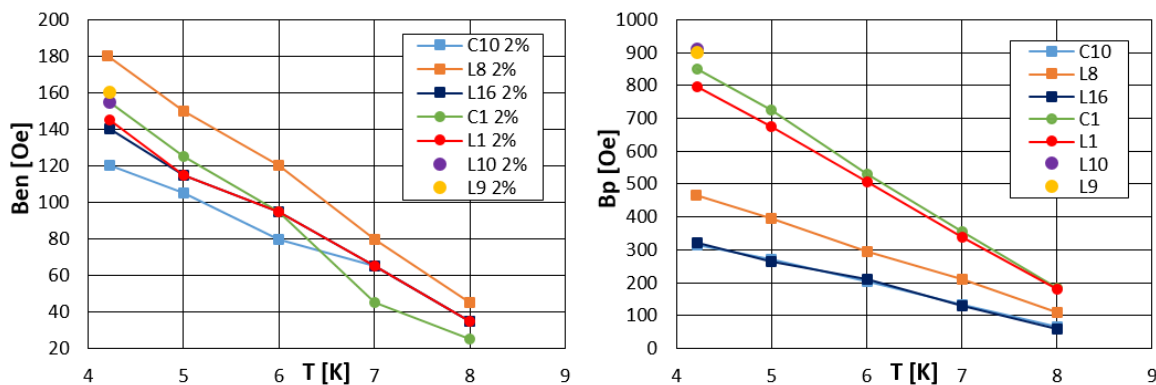


Figure 52 The flux entry field B_{en} (left), determined applying the 2% relative difference criterion, and the field of maximum norm of magnetic moment B_p (right) in dependence on temperature for all the investigated samples. In the case of L10 and L9 only measurements at 4.22 K were performed. [$1 \text{ Oe} = 0.1 \text{ mT}$ (in vacuum), $1 \text{ emu} = 10^{-3} \text{ Am}^2$]

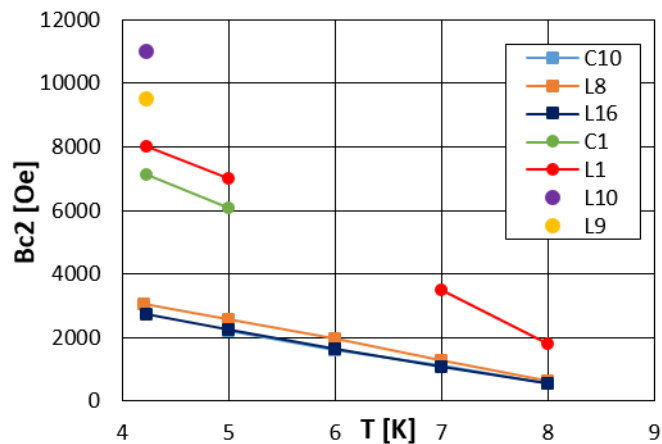


Figure 53 The upper critical field B_{c2} in dependence on temperature for all the investigated samples. In the case of L10 and L9 only measurements at 4.22 K were performed. (Some data points are missing in the trends as those particular measurements did not cover range of applied fields high enough to determine or at least reasonably estimate the B_{c2} value.) [1 Oe = 0.1 mT (in vacuum), 1 emu = 10^{-3} Am²]

5. Discussion

Roughness is known to affect the Q slope on Magnetron sputtered Niobium on copper cavities [12] [13] [14] [15] and Figure 54. Various explanations have been proposed: mainly existence of weak links at grain boundaries related to the granularity of the films, field enhancement on surface features (see next §). In [15], it was noticed that the higher the roughness of the substrate, the higher the density of growth defects (nodule like) is observed.

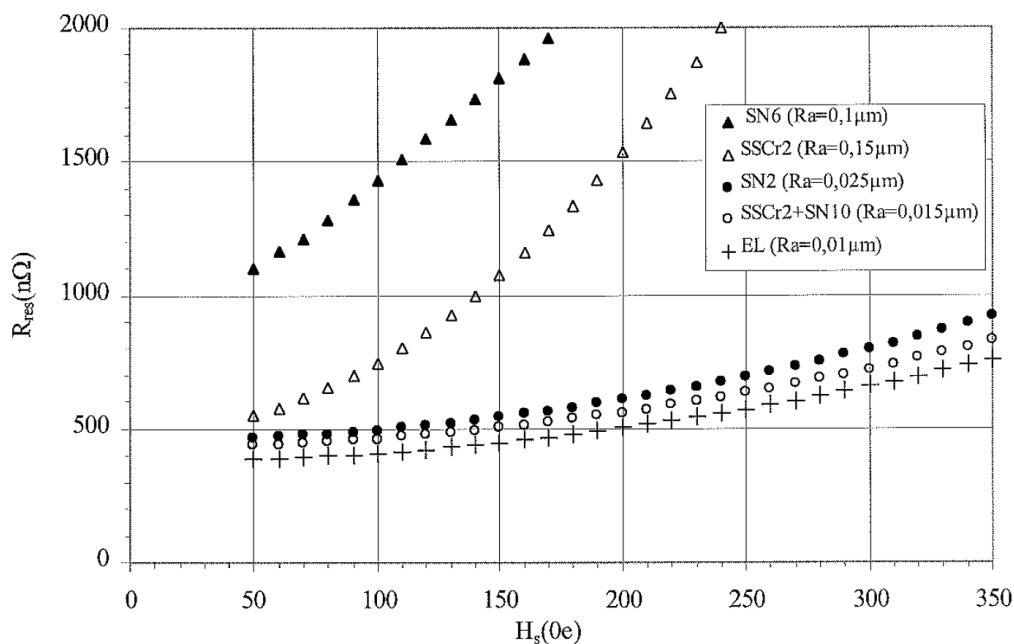


Figure 54 surface resistance in function of the applied RF field for Nb films deposited on copper substrates various roughness [15]

5.1. EXPECTED CONSEQUENCES FROM SURFACE MORPHOLOGY ON RF PERFORMANCE

Summary extracted from [16] and [17].

Roughness

To analyze the impact of roughness it is possible to draw a very simple 2D model as described in Figure 55. For symmetry reason and boundary conditions, the model is symmetric. Here we figure an isolated “bump” with a height h and a width l , and a curvature radius on edges ρ . Note that if $l \gg \rho$ one is featuring a hole instead of a bump, but from the electromagnetic point of view the two situations are equivalent.

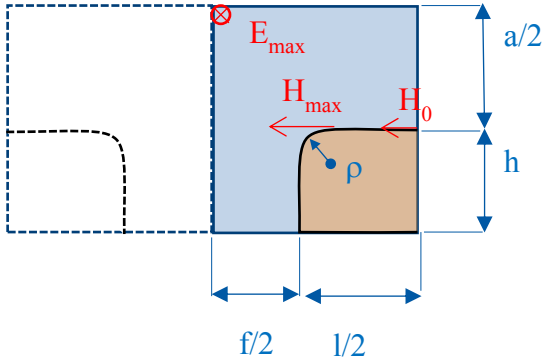


Figure 55 schematic of the EM calculation cell

Within this configuration one can show that :

$$\frac{H_{max}}{H_0} = 1 + 0.266 \left(\frac{f}{l}\right)^{0.3} \left(\frac{f+l}{r}\right)^{0.45}$$

for $0.2 \leq \frac{f}{l} \leq 5$ and

$$\frac{H_{max}}{H_0} = 1 + 0.59 \left(\frac{h}{r}\right)^{0.5}$$

for $0.1 \leq \frac{h}{r} \leq 10$

Figure 56 a) shows the variation of $\frac{H_{max}}{H_0}$ in function of $\frac{h}{r}$ for various geometries and sizes.

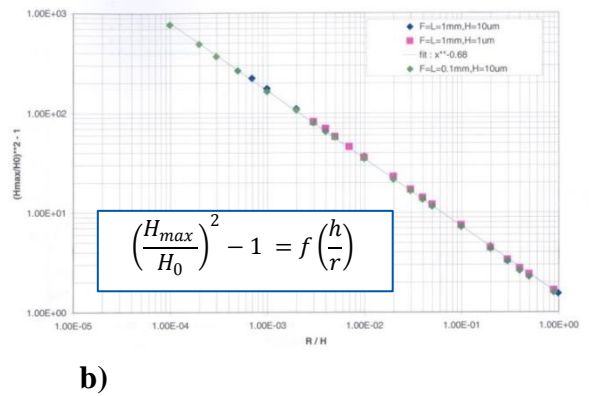
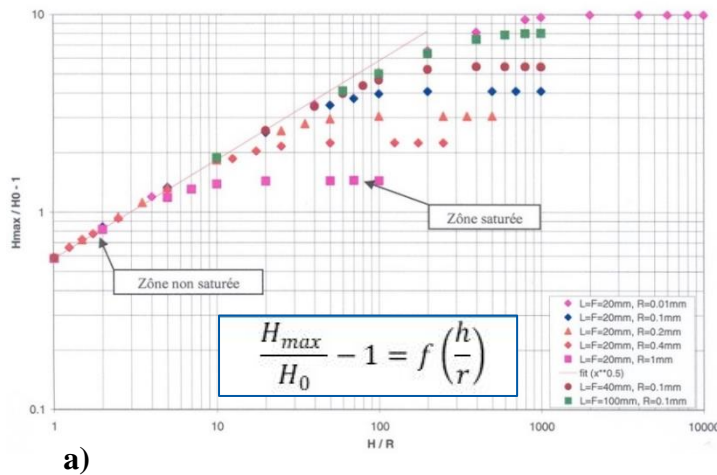


Figure 56 a) $\frac{H_{max}}{H_0} - 1$ as a function of $\frac{h}{r}$, b) $\left(\frac{H_{max}}{H_0}\right)^2 - 1$ as a function of $\frac{h}{r}$ in the saturation regime for various geometries and sizes.

It confirms that any step induces a local increase of the field. When its height h increases (i.e. shape factor increases) one reaches a saturation regime that appears at higher field when the curvature radius on the edge is smaller. The vertical and lateral dimension of the defects do not play a major role on field enhancement, although the lateral dimension affects the total dissipation. The major impact arises from the curvature radius: the smallest the ρ , the higher the field enhancement factor (invert of demagnetization factor). Realistic radius can be inferred from roughness measurement or surface replicas at the μm range. Note that some roughness is also expected at the nm level.

The lateral dimension plays only a minor role compared to the effect of the edge.

Figure 56 b) shows $\left(\frac{H_{max}}{H_0}\right)^2 - 1 = f\left(\frac{h}{r}\right)$ for various geometries in the saturation region, at high field, where the field enhancement factor still increases, but not so rapidly. Figure 56b) shows that field enhancement depends only on the shape factor H/R in this saturation regime for a given ρ .

This model indicates that in fact roughness R_a , which is mostly related to the height h , is only indicative of the issues that might appear in RF. However, we have observed experimentally that the higher the roughness parameter, the higher is the risk to face a morphology defect with a strong impact.

The “sharpness” of the edges can be evaluated with topological tools not available at the moment. Table 9 is extracted from [16] and shows the mean field enhancement factor calculated with Conformal Equivalent Ellipsoids technique for various surface treatment on bulk Nb. For details on this technique see references [16] [17] and references.

Table 9: Roughness parameter and demagnetization factors for ellipsoids measured on standard surfaces

Parameter	Etching (BCP)			Electropolishing (EP)	
	Small-grained material	Annealed, far from the weld	Thermally affected zone (near the weld)	Mean value	Weld defect* $H \sim 50 \mu\text{m}$ $\varnothing \sim 200 \mu\text{m}$
\varnothing grains	70 μm	1–2 mm	0.5–1.0 cm	1 mm \rightarrow 1 cm	-
R_a	1–2 μm	4–8 μm	40–80 μm	$\sim 1 \mu\text{m}$	-
$\beta = 1/D$	1.065	1.028	1.4	1.018	1.9!*

*A defect associated with a hot spot on a cavity quenching at $15 \text{ MV}\cdot\text{m}^{-1}$, observed at Fermilab [18] [19]

One observe indeed small variation on the field enhancement factor, for samples with various surface treatment, grain size and roughness, but this difference keeps below some % unless a large feature is involved. For instance, the effect of BCP/etching on very large grains at the welding seam is important. Those grains are particularly large and well recrystallized and they exhibit sharp edges upon etching. Pitting is also very detrimental, because of the sharp edge on the perimeter of the pit. In conclusion it is very important to prevent the appearance of sharp, large defects like scratches, etching of large and well recrystallized grains (as occurring at welds), and/or etching pits as they can trigger premature quenches. Waviness seems to have a minor role on RF dissipation and early quench.

Other aspects to take into consideration

Thermal conductivity and interface resistance play a paramount role into stabilizing the thermal dissipation that occur locally in the area submitted to higher field. The choice of copper, with its very high thermal conductivity makes sense, but further improvement could arise from the documentation on the thermal resistance that will appear between the SC layer and copper and at the interface with Helium (Kapitza resistance).

6. Conclusions and future work

- Five surface treatments techniques: SUBU, EP, EP+SUBU, Tumbling and Laser Polishing, prepared in 3 different Institutions (CERN, INFN, RTU) on an identical planar substrate
- Different surface characterizations was applied in order to compare the impact of different polishing preparation on copper surface: Roughness, SEM, EDS at INFN.
- A slight difference has been observed between different surface preparations. EP provide a surface pitting free, but the lowest roughness has been obtained with SUBU and tumbling.
- Initial exploration on Laser Polishing shows that it removes larger roughness and scratches, further investigation is required before depositing on.
- 15 samples were coated with minimum 3 μm thick Nb film in DC-MS in 3 different Institutions (STFC, University of Siegen, LNL-INFN).
- Different surface characterizations was applied in order to compare the impact of different polishing preparations on SC films properties: Roughness, SEM, EDS, XRD, AFM, Thermal and Photo Stimulated Exoelectrons, in 4 different institutions (INFN, Siegen, STFC, RTU)
- Superconducting Properties of Nb films were evaluated with PPMS at IEE. It shows a slight difference between deposition facilities rather than different surface preparation; RF test will be required in future to assess the final choice.
- The obtained results are encouraging further exploration on structural and SC characterizations, in order to discover the exact source of variation. This work will continue next year within Task 15.2
- Based on the results of the WP15 first year work, we concluded that the samples for task 15.3, will be prepared by 2 techniques only: EP, as a pitting free technique, and SUBU, as the techniques which provides the lowest roughness without scratches.

References

- [1] S. Stark et al., “Niobium sputter-coated QWRs,” in Proceedings of 8th International Conference on RF Superconductivity (SRF1997), Abano Terme (Padova), Italy, 1997.
- [2] W. Venturini Delsolaro et al., “Nb Sputtered Quarter Wave Resonators for the HIE-ISOLDE,” in Proceedings of 16th International Conference on RF Superconductivity (SRF2013), Paris, France, 2013.
- [3] S. Bauer et al., “Production of Nb/Cu sputtered superconducting cavities for LHC,” in Proceedings of the 9th Workshop on RF Superconductivity, Santa Fe, New Mexico, USA, 1999.
- [4] C. Benvenuti, D. Bloess, E. Chiaveri, N. Hilleret, M. Minestrini, and W. Weingarten, “Superconducting cavities produces by magnetron sputtering of Niobium on Copper,” in Proceedings of 3rd Workshop on RF Superconductivity (SRF1987), Argonne National Laboratory, Illinois, USA, 1987.
- [5] S. Calatroni et al., “Influence of copper substrate treatments on properties of niobium coatings,” in Proceedings of 6th International Conference on RF Superconductivity (SRF1993), CEBAF, Newport News, Virginia, USA, 1993.
- [6] C. Benvenuti, N. Circelli, and M. Hauer, “Niobium films for superconducting accelerating cavities,” *Appl. Phys. Lett.*, vol. 45, no. 5, pp. 583–584, 1984.
- [7] S. Calatroni, “Niobium coating techniques,” *J. Phys. Conf. Ser.*, vol. 114, p. 012006, May 2008.
- [8] J.-P. Birabeau and J. M. A. Guerin, “Patent No 88 09820, Institut National de la Propriété Industrielle, 1993.”
- [9] J. D. Adams, J.-P. Birabeau, J. M. A. Guerin, and S. Pousse, “Procedes de preparation de surface de cuivre compatibles avec un depot de niobium realize par pulverisation cathodique. Presentation d’un bain de polissage chimique repondant a ce critere,” CERN Technical Note 85/SB/AC/B/3199/gp, 1985.
- [10] V. Palmieri, “Fundamentals of Electrochemistry - The Electrolytic Polishing of Metals: Application to Copper and Niobium,” in Proceedings of 11th International Conference on RF Superconductivity (SRF2003), Lübeck/Travemünder, Germany, 2003, 2003.
- [11] H. Padamsee, *RF superconductivity: science, technology, and applications*. Weinheim: Wiley-VCH, 2009.
- [12] S. Calatroni, “20 Years of experience with the Nb/Cu technology for superconducting cavities and perspectives for future developments,” *Phys. C Supercond.*, vol. 441, no. 1–2, pp. 95–101, Jul. 2006.
- [13] V. Arbet-Engels et al., “Superconducting niobium cavities, a case for the film technology,” *Nucl. Instrum. Methods Phys. Res. Sect. Accel. Spectrometers Detect. Assoc. Equip.*, vol. 463, no. 1, pp. 1–8, 2001.
- [14] M. Fouaidy, P. Bosland, S. Chel, M. Juillard, and M. Ribeau, “New results on RF properties of superconducting niobium films using a thermometric system,” in Proceedings of the 8th European Particle Accelerator Conference, Paris, France, 2002.
- [15] M. Ribeau, “Elaboration et caracterisation de films de niobium deposees sur cuivre. Determination de la resistance de surface de supraconducteurs par thermometrie sous vide,” PhD dissertation, Université Paris 6 (France), 1999.

- [16] C. Antoine, "Materials and surface aspects in the development of SRF Niobium cavities," ed. R.S. Romaniuk and J.P. Koutchouk, Vol. 12, 2012.
- [17] C. Z. Antoine, "How to achieve the best SRF performance:(Practical) Limitations and possible solutions," arXiv preprint arXiv:1501.03343, 2013.
- [18] R. E. Ricker and G. R. Myneni, "Evaluation of the propensity of niobium to absorb hydrogen during fabrication of superconducting radio frequency cavities for particle accelerators," J. Res. Natl. Inst. Stand. Technol., vol. 115, no. 5, p. 353, 2010.
- [19] M. Ge et al., "Routine characterization of 3D profiles of SRF cavity defects using replica techniques," Supercond. Sci. Technol., vol. 24, no. 3, p. 035002, Mar. 2011.

Annex: Glossary

Acronym	Definition
SC	Superconductivity
RF	Radio Frequency
SRF	Superconducting Radio Frequency
EP	Electropolishing
QPR	Quadrupole Resonator